TALLINNA TEHNIKAÜLIKOOL
TALLINN UNIVERSITY OF TECHNOLOGY

Department of Materials and Environmental Technology

ONE-STEP CARBON NANOTUBE GRAFTING WITH POLYMER BY REACTIVE MELT BLENDING FOR ELECTROSPINNING OF REINFORCED COMPOSITE MEMBRANES

SÜSINIKNANOTORUDE PINNA KATMINE POLÜMEERIGA ÜHEASTMELISEL KOMPAUNDIMISMEETODIL TUGEVDATUD KOMPOSIITMEMBRAANI TOOTMISEKS ELEKTROKETRUSMEETODIL

MASTER THESIS

Student	Kaia-Kristiina Kirikal
Student code	153434KVEM
Supervisor	Viktoria Vassiljeva

AUTHOR'S DECLARATION

Hereby I declare, that I have written this thesis independently.
No academic degree has been applied for based on this material.
All works, major viewpoints and data of the other authors used in this thesis have been referenced.

"......." .... 201…..

Author: ....
　　　　　　　　/signature /

Thesis is in accordance with terms and requirements

"......." .... 201….

Supervisor: …........................
　　　　　　　　/signature/

Accepted for defence

"......."....................201… .

Chairman of theses defence commission:
....
　　　　　　　　　　　　　　　　　/name and signature/

Table of Content

List of abbreviations

AE   2-aminoethanol

ATRP   Atom transfer radical polymerization

CNT   Carbon nanotubes

DMSO   Dimethyl sulfoxide

DWCNT   Double-Walled Carbon-Nanotubes

FESEM   Field emission scanning electron microscopy

FTIR   Fourier transform infrared spectroscopy

MWCNT-COOH   Multi-walled carbon nanotubes with carboxyl groups

^{1}H-NMR   Nuclear magnetic resonance

p-MWCNT   Pristine multi-walled carbon nanotubes

SAN   Poly(styrene-co-acrylonitrile)

SANm-g-MWCNT   Modified   poly(styrene-co-acrylonitrile)   grafted   multiwalled
                            carbon   nanotubes

SANm   Modified poly(styrene-co-acrylonitrile)

SWCNT   Single-walled carbon nanotubes

$Zn(CH_3COO)_2 \cdot 2H_2O$ Zinc acetate dihydrate

TEM   Transmission electron microscopy

TGA   Thermogravimetric analyses

THF   Tetrahydrofuran

π-π   pi bond

Introduction

Nowadays nanotechnology has attracted more and more interest during last years and carbon nanotube-polymer composites have gained attention from science and industry point of view. Although polymer materials are ideal for forming fibrous materials expeditiously and easily, their mechanical, electrical, thermal, rheological and optical properties need improving. According to the literature, carbon nanotubes (CNTs) can be used for enhancing polymer properties [1].

There are several problems in CNTs functionalization and processing methods. For example, manipulation of MWCNT is limited by aggregation, insolubility and poor dispersion in polymer matrix. Also bad interfacial adhesion between MWCNT and polymer matrix lower efficient load transfer between matrix and MWCNT and mechanical properties decrease. Therefore it is important to find the best solution for functionalization of CNTs [2, 3].

For example, functionalization of CNTs can be conducted with non-covalent bonding and with covalent bonding. With covalent (grafting) chemical bonding of polymer chains to CNTs, strong chemical bonds between nanotubes and polymers are established. With grafting stronger bonds are formed compared to no-covalent modification and also CNTs solubility and dispersion in solvents and in polymers is improved [4].

In this research poly(styrene-co-acrylonitrile) (SAN) was used as a matrix polymer. SAN has good properties such as mechanical properties, heat and chemical resistance [5]. Literature review showed that there are several methods of covalent bonding between SAN and carboxyl group on the surface of the nanotubes, but in this thesis melt blending was chosen due to the method's simplicity and speed. [1, 6, 7, 8]. During this research melt blending method and one-step method for grafting CNTs onto SAN was developed.

With electrospinning can be formed polymer-grafted CNTs nanofibers, which morphology is improved and mechanical properties are enhanced. Good CNT dispersion results in mats with less beads and with decreased fiber average diameter. Dispersion also affects mechanical strength of electrospun fibers positively due to more uniform stress distribution, which leads to the improvement of the matrix polymer's mechanical properties.

This thesis is divided into four main chapters. The theoretical part consists of two chapters in where carbon nanotube–polymer composites are described by explaining their properties, applications, processing and modification methods. The second chapter describes electrospinning process with the parameters that influence the process and the applications of the electrospinning are mentioned. The experimental part consists of used materials and methods and characterization. The experimental part is followed by a section that discusses the results obtained in this study. The very last two sections at this thesis are conclusion and summary.

Objectives

The objective of this research is to form a covalent bond between modified styrene-acrylonitrile (SANm) and multi-walled carbon nanotubes with carboxyl groups (MWCNT-COOH). Through that is improved dispersion of MWCNTs into polymer matrix and electrospun membrane mechanical properties are enhanced as a consequence.

Firstly, SAN is modified using catalyst and after the modification a covalent bond is formed between SANm and carboxyl groups, which is on the surface of multi-walled carbon nanotubes. One-step compounding method was developed for this process.

Secondly, it is proved that the grafting method occurred by conducting thermogravimetric analyses (TGA), nuclear magnetic resonance (^{1}H-NMR), Fourier transform infrared spectroscopy (FTIR) and transmission electron microscopy (TEM) on prepared samples. Solution properties such as electrical conductivity and rheological behaviour are analysed to see if grafting process improved CNTs dispersion.

Finally, electrospinning process is conducted and the mechanical properties and morphology of those mats are analysed in purpose of investigating the effect of grafting on those properties.

1 Carbon nanotube–polymer composites

Carbon nanotube-polymer composites are materials, where carbon nanotubes are used as a reinforcing phase for polymer matrices in purpose of enhancing mechanical and electrical properties of the matrix polymer [1]. At the 1990s by Ajayan the first ever polymer nanocomposites using CNTs as fillers was reported. Since then, there have been many articles dedicated to processing and to the resulting mechanical and electrical properties of polymer nanocomposites [7]. At the time period 1999-2016 there have been 9640 published articles about carbon nanotube-polymer composites. Figure 1 presents published articles by subject area abstracted from Scopus [8].
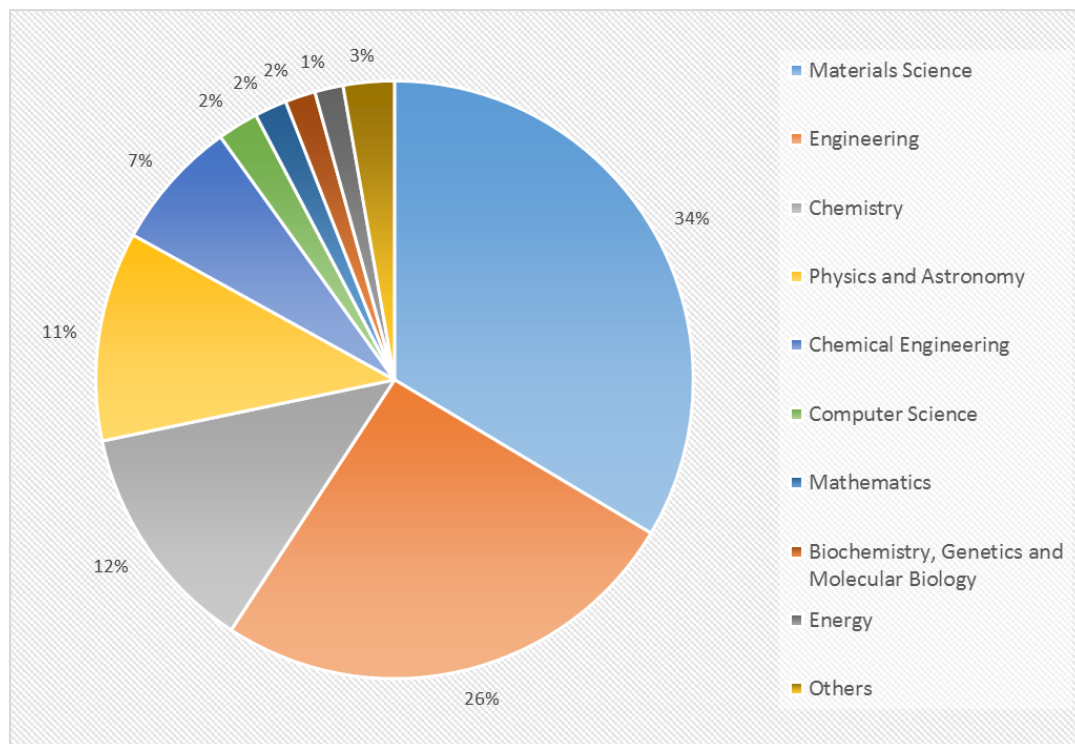
Figure 1. Published articles (1999-2016) about carbon nanotube–polymer composites by subject area [8]

1.1 Carbon nanotubes

Carbon nanotubes have outstanding electrical, mechanical and thermal properties [1]. For example, CNTs have high flexibility, low mass density, large nanotube aspect ratio (typically >1000), high tensile moduli and strength, they also exhibit extraordinary stiffness-to-weight and strength-to-weight ratios [7, 9]. CNTs maximum tensile strength

is approximately 100 GPa, single-walled carbon nanotubes (SWCNT) Young's modulus is 100 GPa and multi-walled carbon nanotubes (MWCNT) have slightly higher value which is 128 GPa. CNTs strain at break is 10% and their electrical conductivity is $10^6 - 10^7$ S/m [10, 11, 12].

Carbon materials can be found in several forms, for example as graphite, diamond, carbon fibers, fullerenes and carbon nanotubes. Carbon atom can form several distinct types of valence bonds and their chemical bonds refer to the hybridization of orbitals by physicists, which is the reason carbon has many structural forms [13].

Carbon nanotubes consist of sheets of hexagonal-shaped carbon atoms, which are rolled up into cylinders. There are three types of carbon nanotube depending on the number of graphite sheet: SWCNT, double walled carbon nanotubes (DWCNT) and MWCNT (see Figure 2) [14].
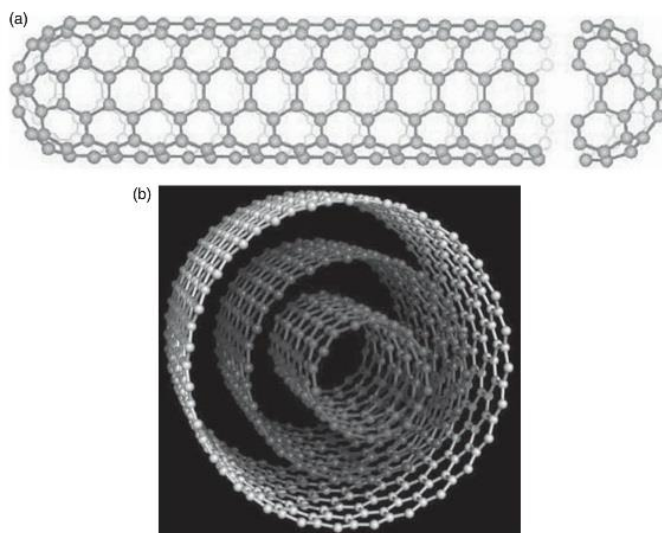
Figure 2. (a) Single-walled carbon nanotube (SWCNT). (b) Multi-walled carbon nanotube (MWCNT) [14]

Depending on the size and structure of nanotube, CNTs can be either semiconducting or metallic. They combine a high modulus with other outstanding mechanical properties. For example, tensile strength can be as high as 63 GPa, which is 50 times higher than the tensile strength of steel. Furthermore, nanotubes have the remarkable ability to recover from deformations. However all nanotubes do not possess exceptional properties. When CNTs are produced catalytically, then most multiwalled tubes have much lower stiffness and strength [15].

Carbon nanotubes have applications in sectors such as automotive, electrical, electronics, sporting goods, renewable energy and drug delivery [14]. Most important uses of CNTs are their applications in sensors and they are also components for lithium ion batteries [15].

Carbon nanotubes cannot be used in its bulk form such as powder, aligned stacks and films/papers due to the poor translation of outstanding inherent properties of individual CNTs into its macroscopic forms. Because of this, the most applications of CNTs involve their combination with other materials in the form of alloys, blends, composites or hybrid materials [16]. CNTs have been used as reinforcement with metal, ceramic and polymer matrix. With composite processing polymers do not damage CNTs and manufacturing cost is reduced. This is the reason why CNT based polymer composites have gained great interests and have been extensively investigated. There are several problems in preparing such composites like how to prepare structure controllable CNTs with high purity and consistently dependable high performance. Another problem is how to break up entangled or bundled CNTs and then uniformly disperse and align them within a polymer matrix. Also there is a problem with improving the load transfer from matrix to CNT reinforcement [17]. The following chapters give an overview of advantages and disadvantages of different modification and processing methods.

1.2 Modification of carbon nanotubes with polymers

The modification of CNTs by polymers can be branched into two main categories: non-covalent and covalent bonding between CNT and polymer. Each branch is divided into sub-branches, which are presented on figure 3 [4].
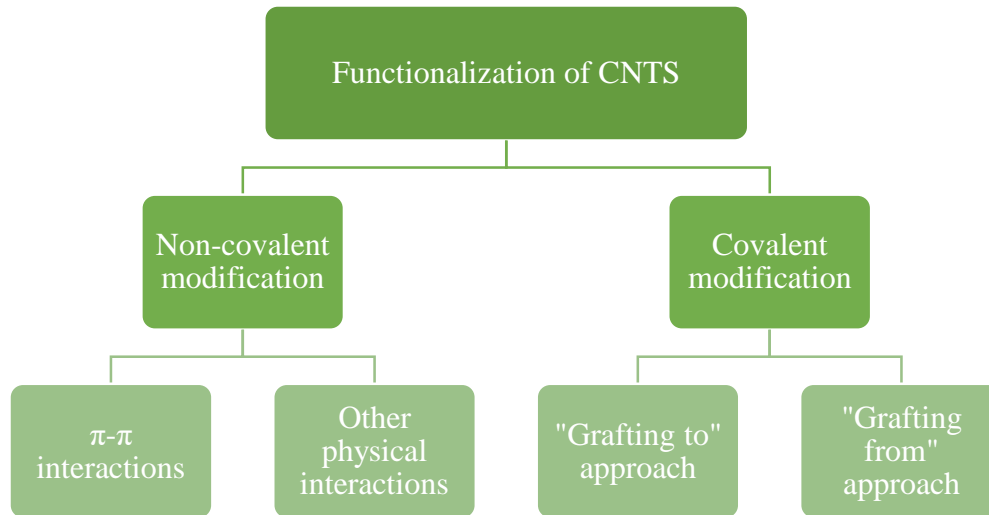

Figure 3. Functionalization of CNTs with polymers [4]

1.2.1 Non-covalent modification

In case of non-covalent CNT modification, there is physical adsorption and wrapping of polymers to the surface of the CNTs. π-π Interaction causes the attachment of small molecular weight polymers or aromatic molecules onto the surface of CNTs [18]. The graphitic sidewalls of CNTs provide the possibility for stacking interactions with conjugated polymers (e.g. polyacetylene, poly(9,9-dialkylfluorene)s, poly(3-alkylthiophene)s, poly(3-octylthiophene)) [7, 19, 20, 21].

The advantage of non-covalent functionalization is that it does not destroy the conjugated system of the CNT sidewalls and does not affect the final structural properties of the material [7]. Therefore, CNTs physiochemical properties are not expected to change significantly [18]. The main disadvantage is that the force between the wrapping molecules and the nanotube might be weak and as a result as a filler in a composite, the efficiency of the load transfer might be low [22].

1.2.2 Covalent modification

In case of covalent chemical bonding (grafting) of polymer chains to CNTs strong chemical bonds between nanotubes and polymers are established [7]. The functionalization of CNT through covalent functionalization is more dominant for improving solubility of nanotubes as well as dispersion in solvents and polymers. Grafting can be carried out either by modification of surface-bound carboxylic acid groups on the nanotubes or by direct reagents to the sidewalls of nanotubes. Functional groups like –COOH or –OH are created on the CNTS during the oxidation in purpose of achieving good dispersion of nanotubes [22]. There are two grafting methods, which are "grafting to" and "grafting from" [4].

The "grafting to" method consists of a synthesis of a polymer with a specific molecular weight terminated with reactive groups or radical precursor. In addition, the polymer chain is attached to the surface of nanotubes by addition reactions [7]. For example, such chemical reactions are radical coupling, amidation, esterification, etc. For chemical reactions the polymer must have suitable reactive functional group. Some polymers that have been used with "grafting to" method are poly(prpionylethylenimine-co-ethylenimine), poly(vinyl acetate-co-vinyl alcohol) and poly(ethylene glycol) [22].

One advantage of the "grafting to" method is that pre-formed commercial polymers of controlled molecular weight and polydispersity can be used [7]. One disadvantage of chemical bonding is that the grafted polymer content is limited because of the relatively low reactivity of macromolecules and only polymers containing reactive functional groups can be used [23]. Another drawback is that initial binding of polymer chains sterically hinders diffusion of additional macromolecules to the CNT surface, leading to a low grafting density [7].

Furthermore, the "grafting from" method involves growing polymers from CNT surfaces via in situ polymerization of monomers initiated by chemical species immobilized on the CNT sidewalls and CNT edges [7, 22]. This polymerization method is an example of reactions called surface-initiated polymerization. For example, surface-derived initiators can be MWCNTs. Initiators are covalently attached using various functionalization reactions developed for small molecules, including acid-defect group chemistry and sidewall functionalization of CNTs [7]. This approach has been used for polymers such

as polyamide 6, polymethyl methacrylate (PMMA), polystyrene (PS), poly(acrylic acid), poly(N-vinylcarbazole), poly(N-isopropylacrylamide), poly(4-vinylpyridine) [22].

Another advantage of "grafting from" method is that the high reactivity of monomers make efficient, controllable, designable and tailored grafting feasible [23]. Also polymer growth is not limited by steric hindrance, which allows high molecular weight polymers to be efficiently grafted [7]. Furthermore, resultant nanotube–polymer composites can exhibit quite high grafting density [22]. Other drawbacks of "grafting from" method are that this method needs strict control of the amounts of initiator and substrate as well as accurate control of conditions required for the polymerization reaction [7].

1.3 Composite processing methods

There are several carbon nanotube-polymer composite processing methods, which are following: melt processing, solution mixing, in situ polymerization and electrospinning [24].

Melt blending is one of the most economical and environmentally friendly methods of processing composites (see Figure 4) [24]. It is a versatile and commonly used method to fabricate polymeric materials, mainly for thermoplastic polymers [25]. The compounding is generally conducted in a single or twin-screw extruder where the polymer and the nanoparticle mixture are heated to form a melt. The mixer imparts shear and elongation stress to the process helping to break apart the filler agglomerates and dispersing them uniformly in the polymer matrix. Better dispersion is achieved with MWCNT than SWCNT [24]. Disadvantages of melt blending are that CNTs can easily be damaged to a certain extent or get broken in some cases and the shear forces generated in most mixing equipment are not large enough to break and disperse the CNT in the polymer matrix efficiently [24, 25]. Advantages of this process method are its speed and simplicity and compatibility with standard industrial techniques [26]. Melt processing also does not require the use of organic solvents during processing and composite can be further processed using other polymer-processing techniques such as injection moulding, profile extrusion, blow moulding [24].
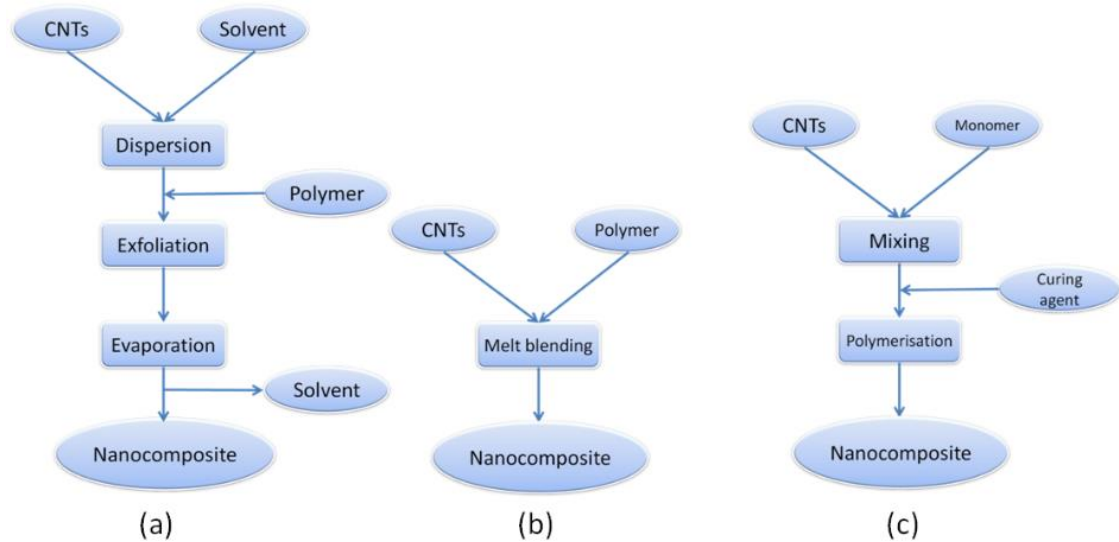
14

Figure 4. Schematic representation of different steps of carbon nanotube-polymer composite processing: solution mixing (a), melt mixing (b), in situ polymerisation (c) [26]

Solution mixing (solvent casting) is another method of producing composites containing nanotubes and polymer (see Figure 4) [24]. CNTs are generally dispersed in suitable solvent and then mixed with polymer solution by mechanical mixing, magnetic agitation or high energy sonication [25, 26]. The carbon nanotube-polymer composites can be formed by vaporizing the solvent at a certain temperature. This method is considered as an effective measure to prepare composites with a homogenous CNT distribution and often used to prepare composite films [25]. With solution mixing can be achieved good dispersion of nanotubes in polymer solutions even when the nanotubes cannot be dispersed in the neat solvent [26].

A variety of CNT-polymer composite has been prepared using in situ polymerization, where both thermoset and thermoplastic materials can be used (see Figure 4) [24]. This method is considered as a very efficient method to significantly improve the CNT dispersion and the interaction between CNTs and polymer matrix. CNTs are mixed with monomers and then carbon nanotube-polymer composites can be obtained by polymerizing the monomers under certain conditions [25]. Advantages of in situ polymerization is that it allows the grafting of polymer molecules on the walls of the tube. The technique is useful in making CNT composites with polymers that are insoluble in most common solvents or are thermally unstable [24].

Another method for composite processing is electrospinning. In purpose of bringing out the anisotropic nature of CNTs, it is important to align CNTs in a polymer matrix during processing of carbon nanotube-polymer composites [24, 25]. The elements of a basic

electrospinning method consists of an electrode connected to a high voltage power supply, which is inserted into a syringe-like container containing the polymeric solution and a collector, where fibers are collected [24].

1.4 Properties and applications of carbon nanotube-polymer composites

The most investigated application of carbon nanotube-polymer composites is the production of composites with advanced mechanical properties. Due to CNTs exceptional stiffness-to-weight and strength-to-weight ratios, together with high ratios of geometric aspect, carbon nanotubes have the potential for being the best possible reinforcing agents in advanced composites [9]. With functionalization, solubility is improved and tendency of agglomeration is reduced [1]. Improved mechanical properties are stiffness, toughness, fatigue resistance, impact resistance, strength and damping [9, 23]. Besides to these improvements, thermal, electrical, optical, dielectric and rheological properties are enhanced as well [16].

The issue of property enhancement is difficult because the improvement in one property might come at the cost of other. Many factors like the nature of the matrix polymer, aspect ratio or actual length/diameter of CNTs, its pretreatment, loading level, exploited processing technique and the presence of tertiary phase (e.g. compatibilizer) can influence the properties of formed nanocomposites [16].

Combination of mechanical and electrical properties of individual nanotubes make these composites the ideal reinforcing agents for following applications: aerospace structures, sporting goods, medicine, sensors, automotive industry, energy storage (see Figure 5) [7, 13, 26, 27, 28, 29].
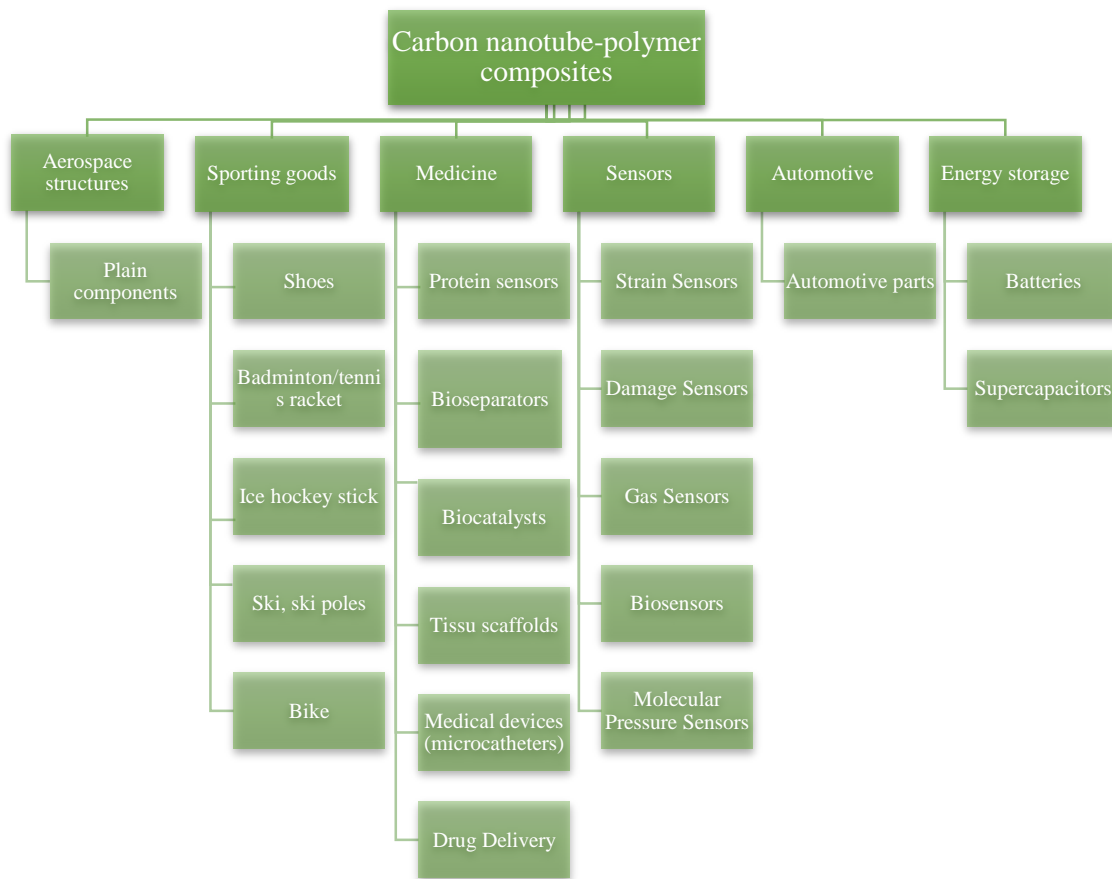
Figure 5. Applications of carbon nanotube-polymer composites [7, 13, 26, 27, 28, 29]

1.5 Carbon nanotube-polymer composites with SAN

SAN has excellent mechanical properties, chemical and heat resistance [5]. Styrene-based materials have unique characteristics of durability, high performance, versatility of design, simplicity of production and economy. They can also provide excellent hygiene, sanitation, and safety benefits. Many products of SAN have very good insulation qualities and the ability to be recycled where collection systems are made available and styrene helps create products that are unique [30].

SAN has importance in several application areas such as automotive, packaging, electronic, and medical applications. Successful grafting of styrene-co-acrylonitrile onto the surface of CNTs can open a route to the fabrication of polymer composites with a fine dispersion of functionalized CNTs [2]. These composites have also a considerably broad potential in coating applications like antistatic coatings and film [6].

There have been several methods of functionalization carbon nanotubes with SAN. According to the literature, the in situ grafting-from approach via atom transfer radical polymerization (ATRP) has been applied to SAN polymer. In this case, grafting process was successful which was made sure using TGA, ^{1}H-NMR and Fourier transform infrared spectroscopy (FTIR). Raman and near-infrared spectroscopy showed that the grafting of SAN slightly affected the sidewall structures. Field emission scanning electron microscopy (FESEM) displayed that CNT surface became rough because of the grafting of the polymers. The polymer-grafted MWCNTs exhibited relatively good dispersion in tetrahydrofuran (THF) [2].

In other article, SAN nanocomposites were prepared by three different methods: pristine MWCNT/SAN by melt blending, P-MWCNT/SAN in situ ATRP and I-MWCNT (2-hydroxyethyl bromoisobutyrate grafted MWCNT)/SAN in situ ATRP. I-MWCNT/SAN in situ ATRP, i.e. SANm-g-MWCNT, showed higher viscosity compared to other nanocomposites, which indicates improved dispersion of MWCNT and interfacial characteristics. Higher tensile properties and toughness and lowest electrical resistance was for SANm-g-MWCNT. These were attributed to the improved interfacial behaviour and degree of dispersion of MWCNT [3].

SAN and MWCNT nanocomposites have been prepared by solution casting from aqueous solution with intensive ultrasound mixing. With this method mechanical, electrical, and thermophysical properties were improved, compared to the pure SAN material [6].

Composites with SAN have also been prepared using reactive melt blending. For this a small amount of cyano groups in SAN was converted to oxazoline groups through reaction with 2-aminoethanol. Reactive melt blending of oxazoline-containing SAN and MWCNTs resulted in the grafting of polymer chains onto MWCNTs. Spectroscopic, thermal and microscopic techniques confirmed the successful grafting of SAN onto MWCNTs. According to the article, this method is comparatively simpler and greener than a previously reported methods and can be adopted to graft other acrylonitrile-containing polymers onto MWCNTs [1].

2 Electrospinning

Electrospinning is a process, where electrostatic force is applied on polymer solution to draw fibers. Nowadays this is a popular method in laboratories to form nanofibers and it also has applications in industries as well. For example, electrospinning is used in industries to manufacture highly efficient filters [31].

2.1 History

William Gilbert was the first person to investigate attraction of a liquid in the seventeenth century. In 1846 Christian Friedrich Schönbein manufactured nitrated cellulose and in 1887 wrote Charles Vernon Boys about producing nanofibers [31]. In 1900 John Francis Cooley was the first to patent electrospinning process [32]. In addition, John Zeleny published work on the behaviour of fluid droplets at the end of metal capillaries in 1914 and after that began attempts to mathematically model the behaviour of fluids under electrostatic forces. During 1931-1944 Anton Formhals implemented 22 electrospinning patents [31]. In 1938 electrospun fibers where used for producing filters [33]. Furthermore, Sir Geoffrey Ingram Taylor gave the beginnings of a theoretical underpinning of electrospinning by mathematically modelling the shape of the Taylor cone, which is formed by the fluid droplet under electric field [31].
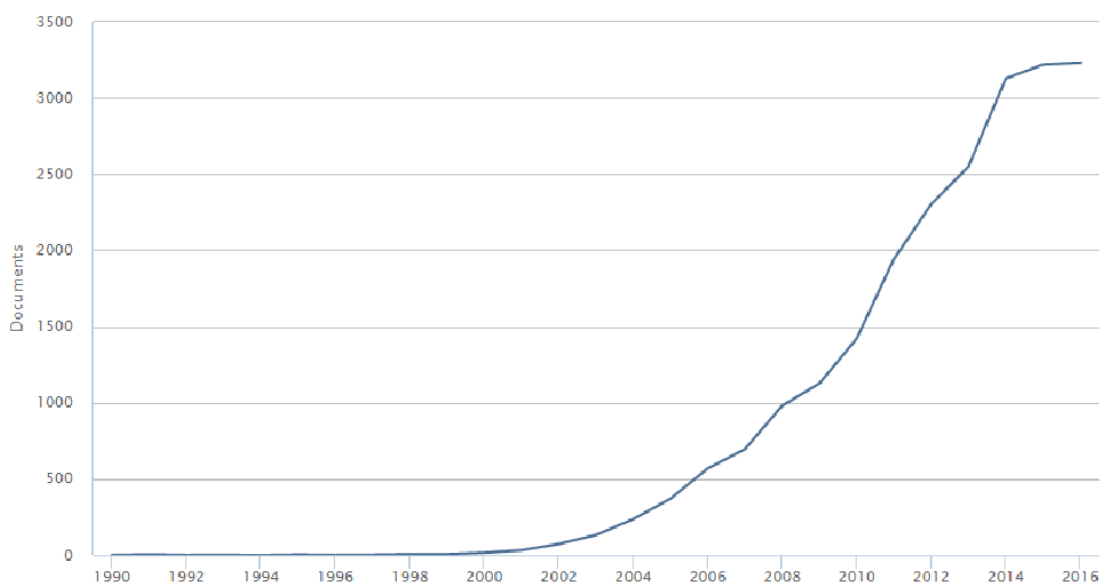

Figure 6. Published articles about electrospinning 1990-2016 [8]

19

In the 1990s electrospinning started to gain more popularity and from that point forward, scientist started to write more articles about the process (see Figure 6) [31]. During past decades, electrospinning has become one important part in nanotechnology, because it is inexpensive method for producing fibers with the size of micro-and nanoscale [34].

2.2 Electrospinning method and apparatus

Spinning equipment has three important components: a high voltage supplier, a needle with small diameter and a collector (Figure 7) [35]. High voltage is used in purpose of creating an electric field between a droplet of polymer solution at the tip of a needle and a collector. One electrode is placed on the needle and the other one is attached to the collector, which is grounded. Due to electric field caused by high voltage supplier, electrically charged jet of polymer solution can erupt from the droplet on the top of the needle. After solvent evaporation, a nonwoven mat of randomly oriented nanofibers is deposited on the collector [36].

The solution in the needle is held by its surface tension. High voltage is applied to the needle and as a result, charge is induced on the surface of the droplet on the top of the needle. A force directly opposite to the surface tension is caused by mutual charge repulsion and the contraction of the surface charges to the counter electrode. Taylor cone is obtained when surface tension has overcome and when jet is obtained. When polymer solution jet undergoes elongation, then the jet becomes thin and long [35].
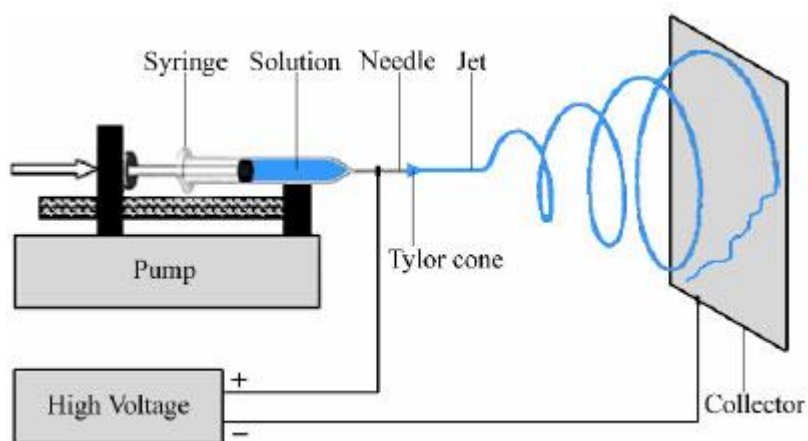

Figure 7. Electrospinning scheme [37]

20

2.3 Electrospinning parameters

Electrospinning process and fiber morphology are influenced by three main parameters: polymer solution parameters, processing conditions and ambient parameters [38].

2.3.1 Polymer solution parameters

Polymer solution parameters such as molecular weight, viscosity, surface tension, electrical conductivity and dielectric effect of solvent have the highest effect on electrospinning process and have significant influence on resultant fiber morphology [38].

Molecular weight, viscosity and surface tension

Polymer solution is thermodynamically stable and molecularly dispersed mixture of polymers and liquids, which have low molecular weight [39]. Molecular weight of a polymer is a measure of the sum of the atomic weights of the atoms in a molecule [40]. Molecular weight influences solution viscosity, because the length of polymer chain determines the amount of entanglement of the polymer chains in the solvent.

Furthermore, when increasing the polymer solution concentration, solution viscosity increases as well. However, the viscosity cannot be too high for several reasons. For example, it is difficult to pump the solution through the syringe needle and solution can also dry at the tip of the needle before electrospinning process starts. Polymer solution should have sufficient viscosity for electrospinning process to occur. Entanglement of the molecule chains prevent electrically driven jet from breaking up during the stretching. As a result, electrospinning solution jet is stable and the process itself is continuous [38].

Solution viscosity has a certain influence on fiber morphology. Beaded fibers are influenced by the instability of the jet of polymer solution. By increasing viscosity, the beads become bigger, the average distance between beads increases, the fiber diameter also increases and as a result the shape of beads change from spherical to spindle-like until smooth fibers are formed. At low viscosity there are beads along the fibers. In case of lower viscosity, there are more solvent molecules and less chain entanglements, which means that surface tension has dominant influence on electrospinning jet, which is the reason for forming beads along the fibers [41].

At higher viscosity, solvent molecules are distributed better along the polymer molecules and beads disappear with the increase of solution concentration. In addition, at high viscosity, there is a bigger interaction between solvent and polymer molecules, because when solution is stretched due to charges, then solvent molecules spread over the entangled polymer molecules [38].

Effect of higher viscosity is reflected also in the smaller deposition area. In case of high solution concentration viscosity is high enough to prevent bending instability at longer distance. Due to that jet path reduces, there is less stretching of the solution and fiber diameter increases. In this case, solvent does not have enough time to evaporate and the fiber melts on the surface of the collector and webs are formed [38].

The diameter of fiber increases with the increase of polymer solution concentration [42]. If there are less charges on the jet and on the solution, then the stretching is weak and due to that the diameter increases [38].

For electrospinning processs to occur, charged solution has to overcome its surface tension. When decreasing surface tension, then beads, which are caused by the contraction of the radius of the jet, decrease steadily [38, 43]

Solution conductivity

Stretching of solution during electrospinning is caused by repulsion of the charges at the surface of the drop at the tip of the needle. When increasing solution electrical conductivity, then electrospinning jet can carry more charges and stretching force towards collector increases as well. Small amount of salts, polyelectrolyte and metal ions can be added to increase electrical conductivity of solution [38, 43]. Due to increased charges there is greater bending instability and deposition area of fibers increases. Because jet path is increased, finer fibers are formed [38].

Most organic solvents are usually known as non-conductive, but still many have sufficient electrical conductivity for electrospinning process to initiate. If a solvent with high conductivity in solution is prepared for spinning, then obtained fibers have no beads, but if solution has zero conductivity, then no fibers are formed, because there is no surface charge at the surface of the fluid droplet to form a Taylor cone [38].

The size of ions influence fiber morphology. If ions have small atomic radius, then they have a greater mobility under an external electrostatic field. As a result, elongational force increases and fibers with smaller diameter are formed [42]. When adding ionic surfactant, then electrical conductivity of solution increases, but surface tension decreases and as a result fiber diameter decreases [38].

Dielectric effect of solvent

The dielectric constant of a solvent has enormous effect on electrospinning process. With higher dielectric constant, there is an increase of bending stability of the electrospinning jet. As a result, there is an increase in deposition area of the fibers and increase in jet path. Diameter and bead formation of resultant electrospun fiber reduces and fiber morphology enhances [38].

2.3.2 Process conditions

Important parameters that affect the electrospinning process are external factors exerting on the electrospinning jet. These are high voltage, feedrate, temperature of the solution, type of collector, diameter of needle and distance between the needle tip and collector. These parameters affect spinning process, however they do not have such enormous effect as solution parameters have [38, 41].

Voltage

High voltage promotes necessary charges on the surface of the solution and if electrostatic force on the solution overcomes the surface tension, then with external electric field it initiates electrospinning process. High voltage is important to achieve stable Taylor Cone. If voltage is higher from the optimum, then the greater amount of charges cause the jet to accelerate faster and more volume of solution is drawn from the tip of the needle. As a result, Taylor Cone is less stable and smaller. With higher voltage, there are great columbic forces in the jet and stronger electric field and this causes greater stretching of the solution. In addition, these parameters reduce the diameter of the fibers and solvent evaporates faster and dry fibers are obtained [38, 41]. Flight time is increased by a lower voltage, the reduced acceleration of the jet and the weaker electric field. Due to long flight time fibers have more time to stretch and to elongate before deposited on the collector. As a result, finer fibers are formed [38].

High voltage also affects the crystallinity of the polymer fiber. The electrostatic field increases the crystallinity in the fiber due to ordered polymer molecules during electrospinning, but above certain voltage value, the crystallinity of fiber is reduced. At high voltage the acceleration of fibers increase and flight time of electrospinning jet is reduced. Because orientation of the polymer molecules takes time, reduced flight time means that the fibers are deposited before the polymer molecules have sufficient time to align themselves. With sufficient flight time, the crystallinity of the fiber improve with higher voltage [38].

Feedrate

Feedrate determines the amount of solution, which is necessary for electrospinning. To maintain stable Taylor Cone, voltage and feedrate have to be corresponding to each other [38]. By increasing the feedrate, the diameter of the fiber increases and the jet dries slower [41]. The residual solvents can cause the fibers to fuse together when they make contact-forming webs. Lower feedrate is preferred, because then the solvent has more time to evaporate [38].

Solution Temperature

When increasing the temperature of the solution, then evaporation rate increases and viscosity of polymer solution reduces. When viscosity is lower, stretching force on the solution is stronger due to Columbic forces. As a result, fibers with smaller diameter are obtained. In addition, with higher temperature polymer molecules mobility increases and Columbic force can stretch the solution further and the diameter of the fiber decreases [38].

Effect of collector

There has to be an electric field between the syringe needle and the collector for electrospinning to occur. Collector is electrically grounded so that there is a stable potential difference between the needle and the collector. If the collector is made of non-conducting material, then charges on the electrospinning jet accumulate on the collector and fibers with lower packing density are obtained. This is caused by the repulsive forces of the accumulated charges on the collector. Honeycomb structure is formed when there is a sufficient density of charges on the fiber mesh. In case of conducting collector,

charges on the fibers are dissipated and fibers with bigger packing density are drawn on the collector. But when the deposition rate is high and if the fiber mesh is thick, high accumulation of residual charges occurs on the fiber mesh, because polymer fibers are usually non-conductive. This results in the formation of dimples in the fiber mesh [38]. With less conductive collector deposited fibers retain some of their charges and incoming fiber is repelled and fiber deposition and productivity are reduced as well [44].

Porosity of the collector affects the packing density of the fibers. High porosity on the porous surface causes faster evaporation of residual solvents. Due to slow evaporation rate there is an accumulation of solvents around the fibers on smooth surfaces and fibers are pulled together to form densely packed structure. On porous collector fibers dry faster and on the fibers remain the residual charges, which will repel subsequent fibers. In addition, on a smooth surface, the residual solvents will encourage the residual charges to be conducted away to the collector [38].

Electrospinning process is influenced by the collector type – if it is static or moving. Rotating collector is used for forming aligned fibers. This collector is suitable for electrospinning solutions, which evaporation is low. In addition, there is more time for solvent to evaporate and drier fibers are obtained [38].

Diameter of needle

The internal diameter of the needle reduces the clogging and the amount of beads on the fibers. Reduction in the clogging occurs, because there is less exposure of the solution to the atmosphere during electrospinning. Furthermore, in case of needle with small internal diameter, there is a reduction in the diameter of the fiber and the size of the droplet at the tip of the needle decreases and the surface tension of the droplet increases. For the same voltage applied, a greater columbic force is necessary to cause jet initiation. Due to that, the acceleration of the jet decreases and this allows more time for the solution to be stretched and elongated before it is collected [38].

Distance between tip of the needle and the collector

Flight time and electric field influence the electrospinning process and the morphology of resultant electrospun fibers [43]. By changing the distance between the tip of the needle and the collector, the flight time and electric field strength are influenced as well. In

purpose of forming fibers, it is important that the electrospinning jet would have enough time for the solvents to be evaporated. By reducing the distance between the tip of the needle and the collector, the electric field strength also increases and this increases the acceleration of the jet to the collector. As a result, there is not enough time for the solvent to evaporate and the resultant fiber needs additional drying before usage. When the distance between the tip of the needle and the collector is increased, then flight time increases and there is more time for the solution to be stretched before it is deposited on the collector. Furthermore, in case of bigger distance, fiber diameter can increase, because electrostatic field strength decreases and stretching of the solution decreases. However, if the distance is too big, then no fibers are deposited on the collector [38].

2.3.3 Ambient parameters

The effect of surrounding environment on electrospinning process is rather poorly investigated. Fiber morphology can be influenced by any interaction between the surrounding and the polymer solution [43]. Ambient parameters are for example humidity, type of atmosphere, temperature, pressure and vacuum [38].

Humidity

Humidity of the environment can influence the morphology of fibers if the polymer is dissolved in volatile solvents. At high humidity in atmospheric spinning conditions, water condenses on the surface of the fiber. Also circular pores are formed on the fiber surface. At higher humidity bigger circular pores are formed and with increasing humidity they increase until non-uniform shaped structures are attained [38].

The humidity of the environment also influences the rate of evaporation of the solvent in the solution during electrospinning [43]. At low humidity, volatile solvents evaporate rapidly. The evaporation of the solvent can be faster than the removal of the solvent from the tip of the needle and this can cause clogging of the needle [38].

Type of atmosphere

Electrospinning process is influenced by the composition of the air in the environment. Different gases behave differently under high electrostatic field. For example, helium breaks down under such conditions and spinning is not possible. When using gases, which have higher breakdown voltage, such as dichlorodifluoromethane, then the fibers

26

obtained have twice the diameter of those electrospun in air given all other conditions equal [38].

Pressure

Under enclosed conditions, it is possible to examine the effect of pressure on the electrospinning jet. Reduction in the pressure surrounding the electrospinning jet does not enhance the electrospinning process. If the pressure is below atmospheric pressure, the polymer solution in the syringe has greater tendency to flow out of the needle and there causes unstable jet initiation. With decreasing pressure, there is rapid bubbling of the solution at the needle tip. In addition, at very low pressure, electrospinning is not possible due to direct discharge of the electrical charges [38].

2.4 Applications of electrospun nanofibers

Electrospun fibers have large surface area, high tensile strength and low density. With this method, porous fibers can be formed and the method itself is inexpensive. Due to excellent physical properties, nanofibers have several uses, which are filter media, nano-sensors, military protective clothing, cosmetic skin mask, tissue engineering scaffolding and has applications in life science (see Figure 8) [35].
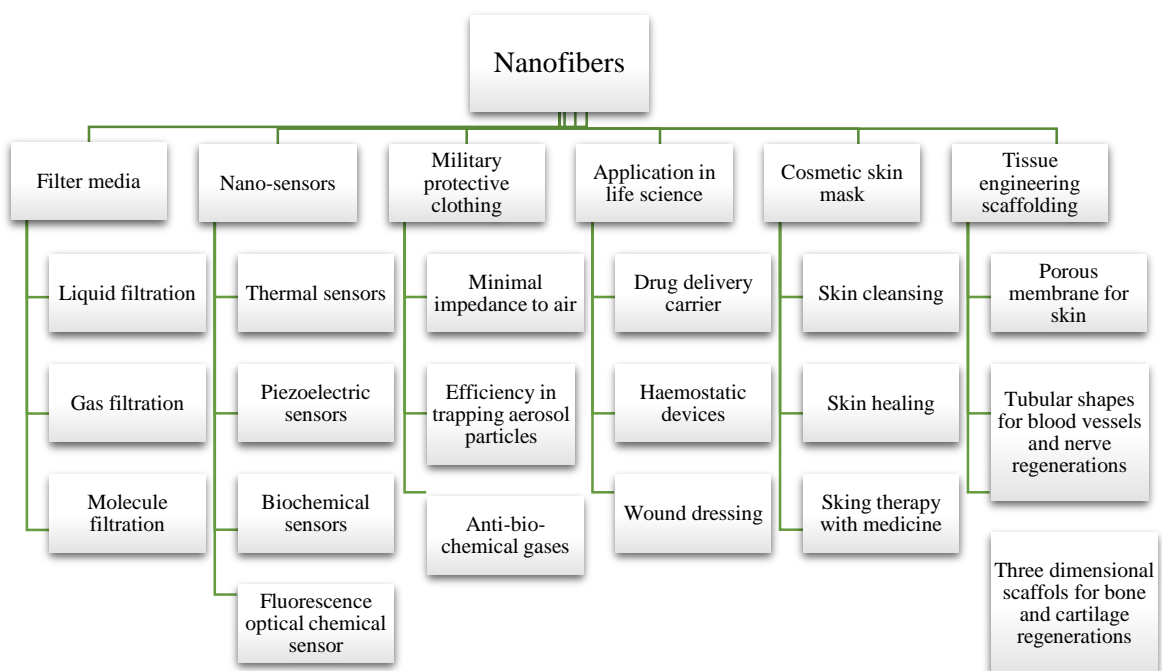

Figure 8. Applications of electrospun nanofibers [35]

3 Experimental part

3.1 Materials and methods

3.1.1 Preparation of SANm-g-MWCNT with one-step compounding method

5,4 mg of zinc acetate dihydrate ($Zn(CH_3COO)_2 \cdot 2H_2O$) (EMSURE®, Germany) was added to 0,45 g of 2-aminoethanol (AE) (Merck Millipore, Germany). Then the mixture was ultrasonically mixed (BANDELIN electronic GmbH & Co. KG) for 10 minutes with cycle 7 and nozzle MS-73 was used (Figure 9).
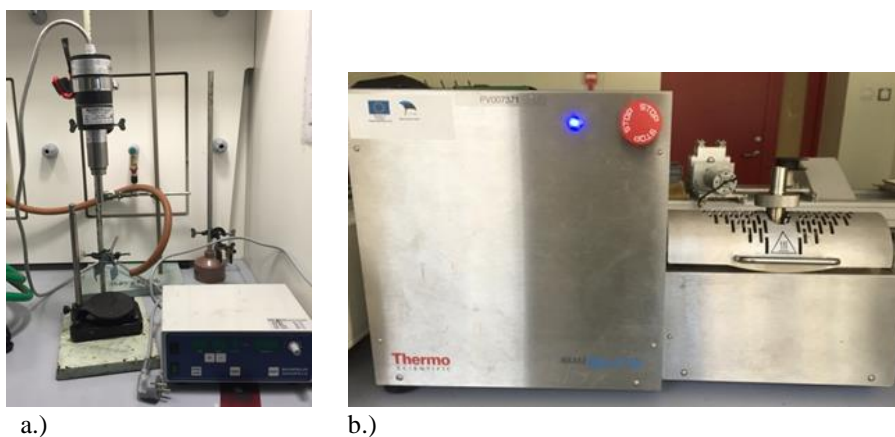

a.) b.)

Figure 9. a.) BANDELIN electronic GmbH & Co. KG b.) HAAKE MiniCTW

4,5 g of SAN (Polimeri Europa SRIL, Italy) was fed into a mixing moulder HAAKE™ MiniCTW Micro-Conical Twin Screw Compounder (Thermo Scientific, USA) (see Figure 9) at 150 °C and a mixture of 0,45 g of AE and 5,4 mg of $Zn(CH_3COO)_2 \cdot 2H_2O$ was added to SAN powder. Then the mixture was mixed at 150 °C for 10 minutes at rotating speed at 80 rpm. After that, the mixture was blended for 20 minutes at 200 °C. The purpose of this process was to convert cyano groups into oxazoline groups. After reaction took place, 0,1 g of MWCNT-COOH (average diameter 8-15 nm, average length 0.5-2.0 μm, purity 95 wt%) (Cheap Tubes, USA) was fed into the compounder and mixed for another 30 minutes at 200 °C. The SANm-g-MWCNT was then extruded from the compounder. On figure 10 there is presented a reaction for grafting of SAN onto MWCNTs.

Then the resulting material had to be washed to eliminate ungrafted substances. For this, the extruded material (weight 3,7 g) was dissolved in 100 ml of THF (Honeywell Riedel-de Haen®, Israel) (see Figure 11). Then the mixture was stirred mechanically for one
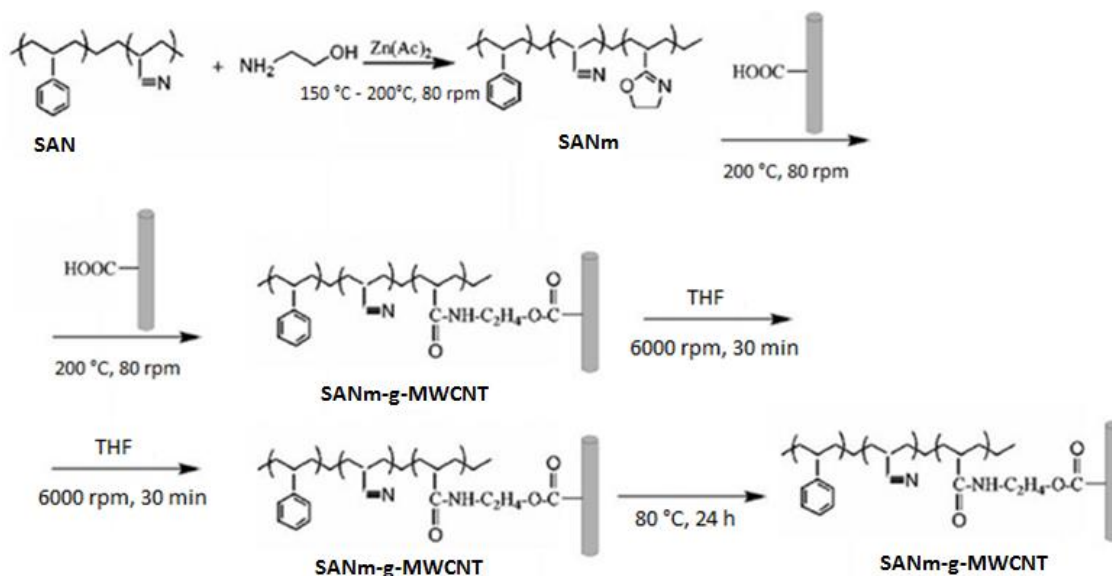
Figure 10. Grafting of SAN onto MWCNTs [1]

hour and centrifuged with Hettich® EBA 21 centrifuge (Hettich®, Germany) at 6000 rpm for 30 minutes. Centrifugation was repeated for several time until transparent centrifugate was obtained. Each time another 100 ml of THF was added to the precipitate. Centrifugate was afterwards re-centrifuged to attain the rest of SANm-g-MWCNT from the first centrifugate. Finally, the samples were put in the vacuum oven for 24h at 80 °C. The yield of the process was 55%.
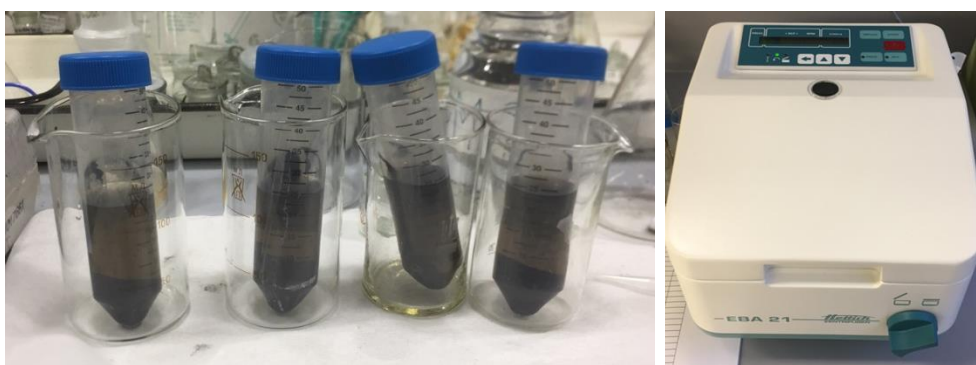

Figure 11. Mixture of SANm-g-MWCNT and THF in Falcone tubes and Hettich® EBA 21 centrifuge

3.1.2 Preparation and filtration of SANm

For Fourier transform infrared spectroscopy analysis, modified styrene-acrylonitrile (SANm) was prepared. SAN was compounded with AE and $Zn(CH_3COO)_2 \cdot 2H_2O$ mixture to modify the polymer. For this procedure, 4,5 g of SAN was fed into a mixing molder at 150 °C and a mixture of 0,45 g of AE and 5,4 mg of $Zn(CH_3COO)_2 \cdot 2H_2O$ was added to SAN powder. Then the mixture was mixed at 150 °C for 10 minutes at rotating

speed at 80 rpm. Then the mixture was blended for 20 minutes at 200 °C. Finally, the oxazoline-modified SAN was extruded from the compounder.

SANm was filtered to ensure the complete removal of $Zn(CH_3COO)_2 \cdot 2H_2O$ residue. 1,05 g of extruded SANm was dissolved in 10 ml of THF by mechanical mixing for 45 minutes. Furthermore, SANm dissolved in THF was precipitated with 300 ml of methanol (Honeywell Riedel-de Haen®, Germany) (see Figure 12). Then the mixture was put under filtration system and filtered with 0,45 µm pore size PTFE filters (Sartonus Stedim Biotech Gmbh, Germany). For solvent evaporation, the modified polymer was dried in a vacuum oven for 24 h at room temperature. The yield of this process was 79%.
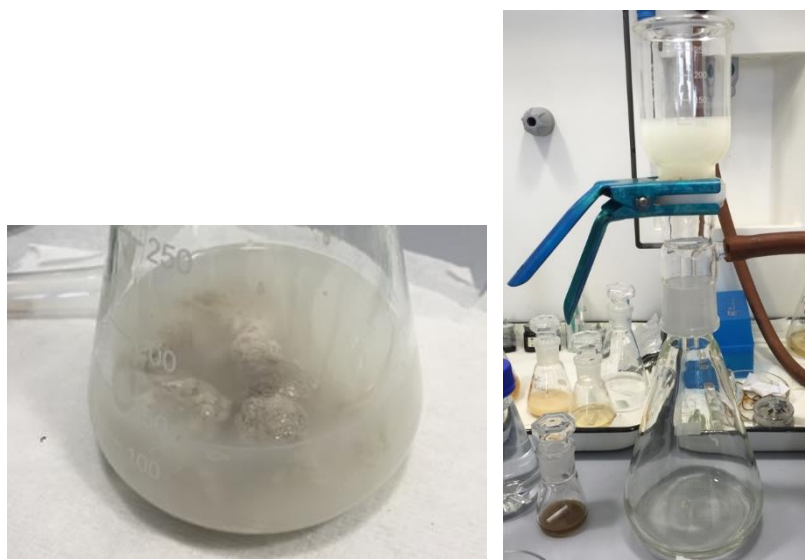

Figure 12. Perticipate of SANm and filtration system

3.1.3 Electrospinning solutions preparation

Different polymer solutions were prepared for electrospinning and for electrical conductivity and rheology analyses:

- 20% SAN in DMSO
- 20% SAN in DMSO + 1% MWCNT
- 20% SAN in DMSO + 1% MWCNT-COOH
- 20% SAN in DMSO + 1% SANm-g-MWCNT

The solutions were mechanically mixes for 24 hours at 60 ºC. The quantity of polymer was calculated according to the formula:

$$C = \frac{weight\ of\ polymer}{weight\ of\ polymer\ +weight\ of\ solvent} \cdot 100\% \qquad (1)$$

Where C is the concentration of solution (%).

The quantity of MWCNT was calculated according to the formula:

$$C = \frac{weight\ of\ carbon\ nanotubes}{weight\ of\ polymer} \cdot 100\%$$

3.2 Characterization

3.2.1 Thermogravimetric Analysis

Thermogravimetric analysis (TGA) was performed in Department of Materials and Environmental Technology at Laboratory of Inorganic Materials. Experiments were conducted on SAN, SANm, MWCNT-COOH and SANm-g-MWCNT with one-step method. The experiments with a Setaram LabsysEvo 1600 thermoanalyzer coupled with Pfeiffer OmniStar Mass Spectrometer by a heated transfer line are carried out under non-isothermal conditions by heating up to 800 ºC at the heating rate of 10 °C min^{-1} in an atmosphere of argon. Standard 0,1 mL aluminium oxide crucibles were used, the mass of the samples was 4-5 mg and the gas flow was 60 mL min^{-1}.

3.2.2 Nuclear Magnetic Resonance

Nuclear magnetic resonance (^{1}H-NMR) spectrum was carried out in University of Helsinki at Department of Chemistry on SANm-g-MWCNT with one-step method. ^{1}H-NMR spectrum were recorded with a Bruker Avance III spectrometer operating at 500 MHz for protons. Sample (7 mg/ml) was first dispersed in d6-DMSO by keeping it at 50 °C overnight followed by vortex mixing for several minutes. The spectra was collected at room temperature with 32 scans.

3.2.3 Fourier transform infrared spectroscopy

FTIR spectra were recorded with Interspec 200-X FTIR spectrometer (Figure 13), with 16 scans averaged at resolution of 1 cm^{-1} for SAN and SANm.

Figure 13. Interspec 200-X

3.2.4 TEM

TEM measurements were performed at Tartu Univesrity Institute of Physics and done with FEI Titan Themis 200 working at 80 kV.

3.2.5 Electrospinning

For electrospinning was used high voltage supplier (Ormond Beach, FL, USA), syringe pump (NewEra Pump Systems, Inc, USA) with 3 milliliter syringes, which inner diameter is 10 mm and diameter of needle is 0,6 mm.


Figure 14. Electrospinning apparatus

Fiber was collected to a rotational drum, which was used as the collector and it was covered with foil paper (Figure 14). Electrospinning parameters were following: voltage 20 kV, distance between the collector and the needle 20 cm, feedrate 0,5-0,6 ml/h.

3.2.6 Analyses of solution properties

Electrical conductivity measurements were conducted with Mettler Toledo electrical conductivity meter (Mettler-Toledo International Inc, USA) at 24.2-25.3 °C. Viscosity measurements were done with Physica mcr 501 rheometer (Anton Paar, Austria) at 23 °C between shear rates 0,01-100 1/s using plate and cone combination with angle 2° and diameter 2,5cm (Figure 15).
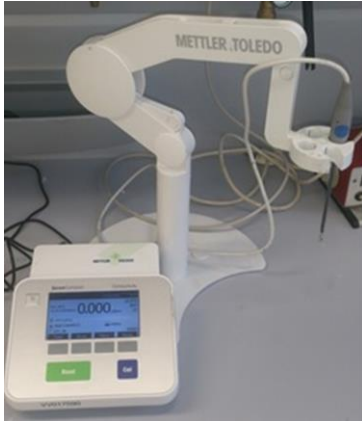
a.)   b.)

Figure 15. a.) Mettler Toledo electrical conductivity meter, b.) Physica mcr 501 rheometer

3.2.7 Tensile testing

Tensile tests were conducted with a tensile testing machine Instron 5866 (see Figure 16). Tensile tests were performed on following mats: SAN, SAN + 1% MWCNT, SAN 1% MWCNT-COOH and SAN + 1% SANm-g-MWCNT. For sample preparation, mats were cut in a rectangular shape (length 100 mm and width 1 mm) and thickness of specimen was measured with digital thickness gage (INSIZE CO., LTD.) For tensile testing a 2,5 kN load cell with strain rate of 100 mm/min was used.

Figure 16. Tensile testing machine Instron 5866

4 Results and discussion

4.1.1 Characterization of SANm-g-MWCNT

4.1.2 Fourier transform infrared spectroscopy

To prove if modification of SAN occurred, FTIR was conducted on SAN and SANm. Figure 17 represents FTIR spectrum and it can be noted that at peak 1601cm^{-1} SAN and SANm have C=C vibration band of styrene units and at 2237cm^{-1} there is C≡N bond of acrylonitrile functional group [1, 45]. SANm spectra exhibits peak at 1664 cm^{-1}, which represents oxazoline functional group. This peak shows that cyano groups of SAN were successfully converted into oxazoline groups of SANm. [1].
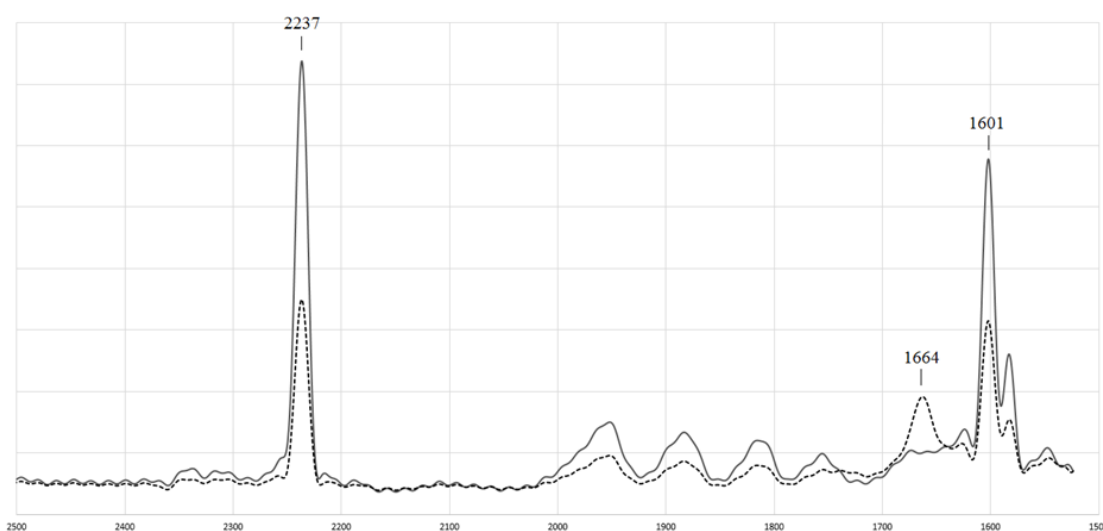

Figure 17. FT-IR spectra of SAN (solid line) and SANm (dotted line)

4.1.3 Nuclear Magnetic Resonance

^{1}H-NMR was used to analyse SANm-g-MWCNT in purpose of verifying the reaction between SANm and MWCNT-COOH. Figure 18 represents the spectrum of SANm-g-MWCNT. Solvent peaks are marked with an asterisk. Material exhibits peaks at 6,84 and 7,17 ppm, which are aromatic protons from styrene unit [1]. ^{1}H-NMR spectrum shows peaks at 0,87 and 1,26 ppm, which come from impurities. According to the literature review, DMSO can cause these signals [70]. Furthermore, for ^{1}H-NMR analysis should be chosen solvent that is more compatible so that solvent peaks would not overlap with peaks of acrylonitrile peaks around 2,0-3,5 ppm. The signal from styrene units in the

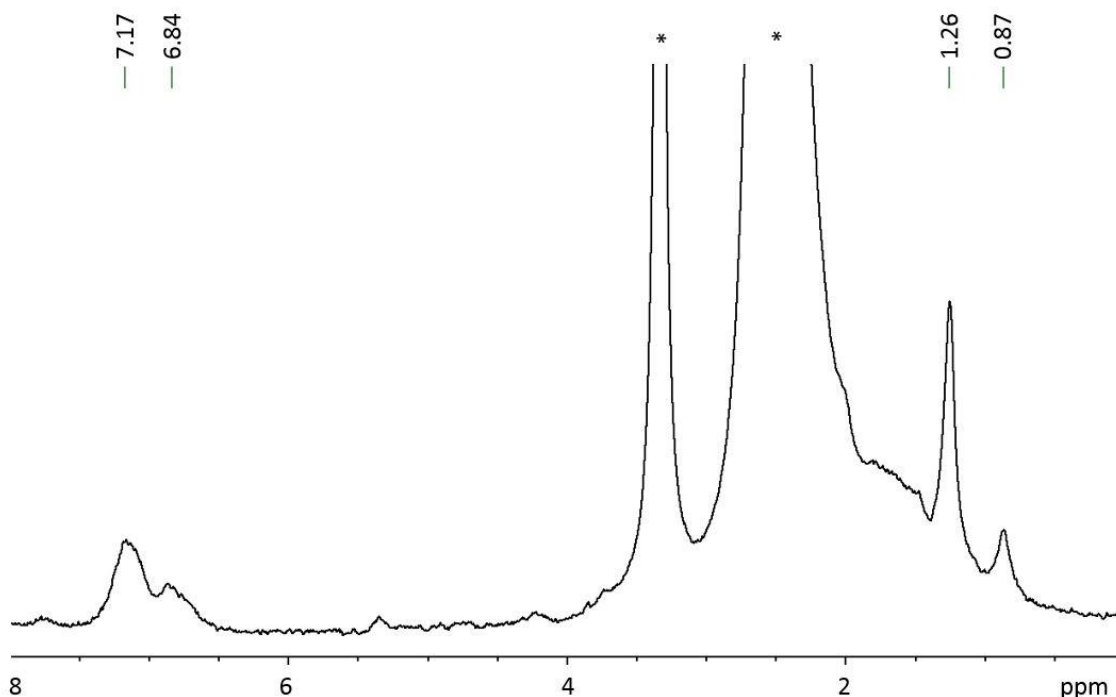sample mean that the grafting reaction was successful and that SAN is present in the sample.

Figure 18. ¹H-NMR spectrum of SANm-g-MWCNT

4.1.4 Transmission electron microscopy

Transmission electron microscopy (TEM) was used to analyse the morphology of SANm-g-MWCNT. On figure 19 it can be seen that material exhibits a core-shell structure, which is composed of nanotube core and outer shell is polymer [1]. This means that CNTs are covered by the matrix polymer and the grafting process was successful.
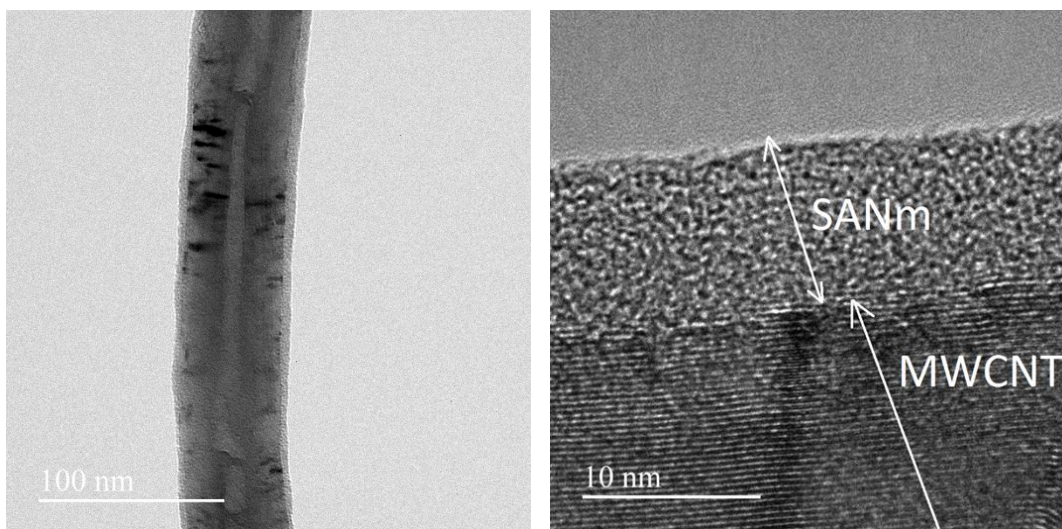

Figure 19. TEM of SANm-g-MWCNT

4.1.5 Thermogravimetric Analysis

TGA was conducted to find out the amount of SAN grafted onto carbon nanotube surface and to characterize the thermal behaviour of SAN, SANm, MWCNT-COOH and SANm-g-MWCNT (Figure 20). From that graph, it can be seen that SAN begins to decompose at 380 °C and loses its weight completely at 420 °C. Although SANm curve is similar to SAN curve, SANm starts to decompose at 360 °C, but loses mass completely at the same temperature as SAN does. Polymer mass loss of 100% is related to the purity of the polymer material. From the literature review, it can be concluded that from other TGA of SAN, the results are similar [1, 46].
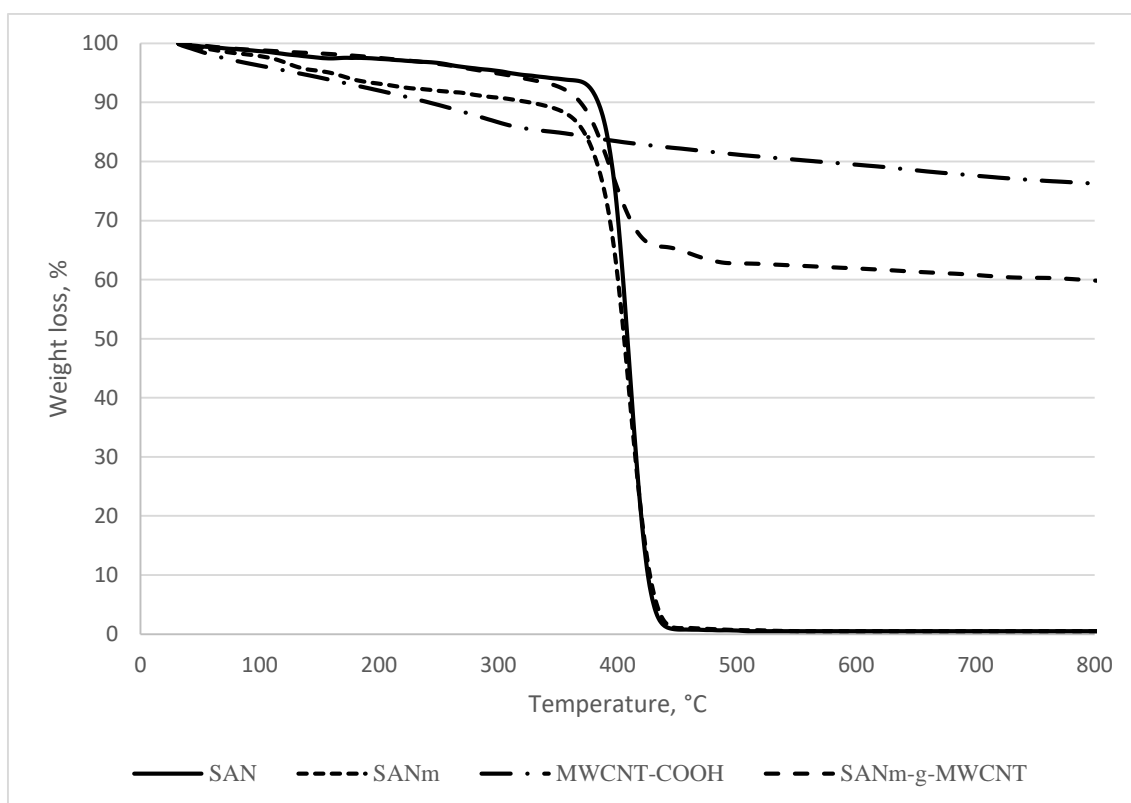

Figure 20. TG mass loss curves

From the graph, it can be noted that in case of MWCNT-COOH curve, there is a continuous decomposition with the increase of temperature. The mass loss results from the decomposition of the carboxyl functional groups introduced onto the surface of MWCNTs [1, 47].

In addition, in case of SANm-g-MWCNT, material loss is 40% and it occurs between 380-430 °C, which is close to the decomposition temperature of SAN copolymer. Literature review shows also similar TGA analyses results [1].

36

4.2 Solution properties

In purpose of investigating effect of grafting reaction on solution properties, electrical conductivity and rheological behaviour of solutions were examined.

4.2.1 Solution electrical conductivity

Figure 21 shows results of electrical conductivity measurement of 20% SAN in DMSO, 20% SAN in DMSO + 1% MWCNT, 20% SAN in DMSO + 1% MWCNT-COOH, 20% SAN in DMSO + 1% SANm-g-MWCNT solutions.

20% SAN in DMSO solution has the lowest conductivity, which is 0,84 µS/cm. This is because SAN is non-conductive polymer and the solvent causes the electrical conductivity of a polymer solution [48]. Electrical conductivity of pure DMSO is 0,92 µS/cm.
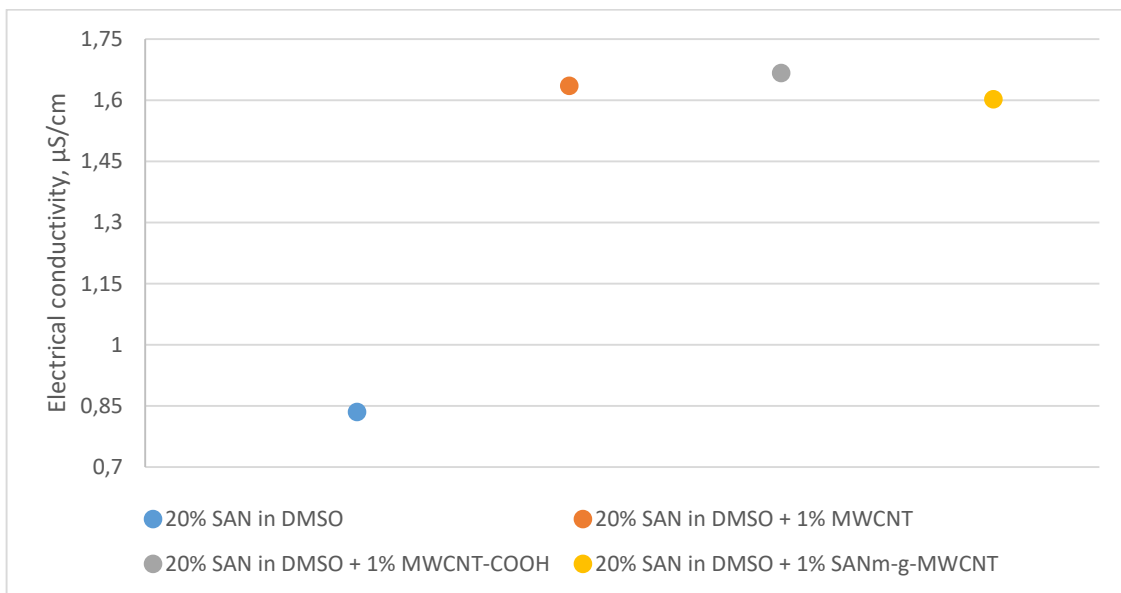

Figure 21. Solution electrical conductivity

In addition, the highest electrical conductivity measured was 1,67 µS/cm, which is the conductivity of 20% SAN in DMSO + 1% MWCNT-COOH solution. In addition, electrical conductivity of 20% SAN in DMSO + 1% MWCNT solution is 1,64 µS/cm. Solutions with carbon nanotubes have higher electrical conductivity than pure polymer solution, because CNTs have excellent electrical properties and therefore improve electrical conductivity of polymer solution, when they are dispersed into the polymer solution [1, 49].

There is a difference in electrical conductivity between MWCNT and MWCNT-COOH, because electrical properties are sensitive to the degree of functionalization and to the chemical nature of the functional group [50]. When the CNTs are modified with carboxylic anion groups, the dispersion stability in polar solvents enhance due to the combination of polar–polar affinity and electrostatic repulsion and this results in better conductivity of 20% SAN in DMSO + 1% MWCNT-COOH solution compared to the solution with MWCNT [51].

20% SAN in DMSO + 1% SANm-g-MWCNT solution electrical conductivity is 1,60 µS/cm. With SANm-g-MWCNT dispersion into polymer solution, there is also an increase of electrical conductivity compared to pure polymer solution due to excellent conductivity of CNTs. However, compared to the conductivity of solutions composed of MWCNT and MWCNT-COOH, electrical conductivity of 20% SAN in DMSO + 1% SANm-g-MWCNT solution is slightly smaller. This is caused by the grafting process, where CNTs are covered with the polymer.

4.2.2 Rheology of solutions

On figure 22 can be seen flow curve of 20% SAN in DMSO, 20% SAN in DMSO + 1% MWCNT, 20% SAN in DMSO + 1% MWCNT-COOH, 20% SAN in DMSO + 1% SANm-g-MWCNT solutions.

On figure 22 and figure 23, it can be noted that by applying bigger energy, then structure breaks into smaller domains. When applying bigger shear rate, then the structure breaks apart and the viscosity decreases. Polymers have long entangled molecular chains. With increasing shear rates chain-type molecules in a solution can distangle, stretch and orient themselves parallel to the driving force. Molecular alignments allow molecules to slip past each other more easily and viscosity is decreased [52].
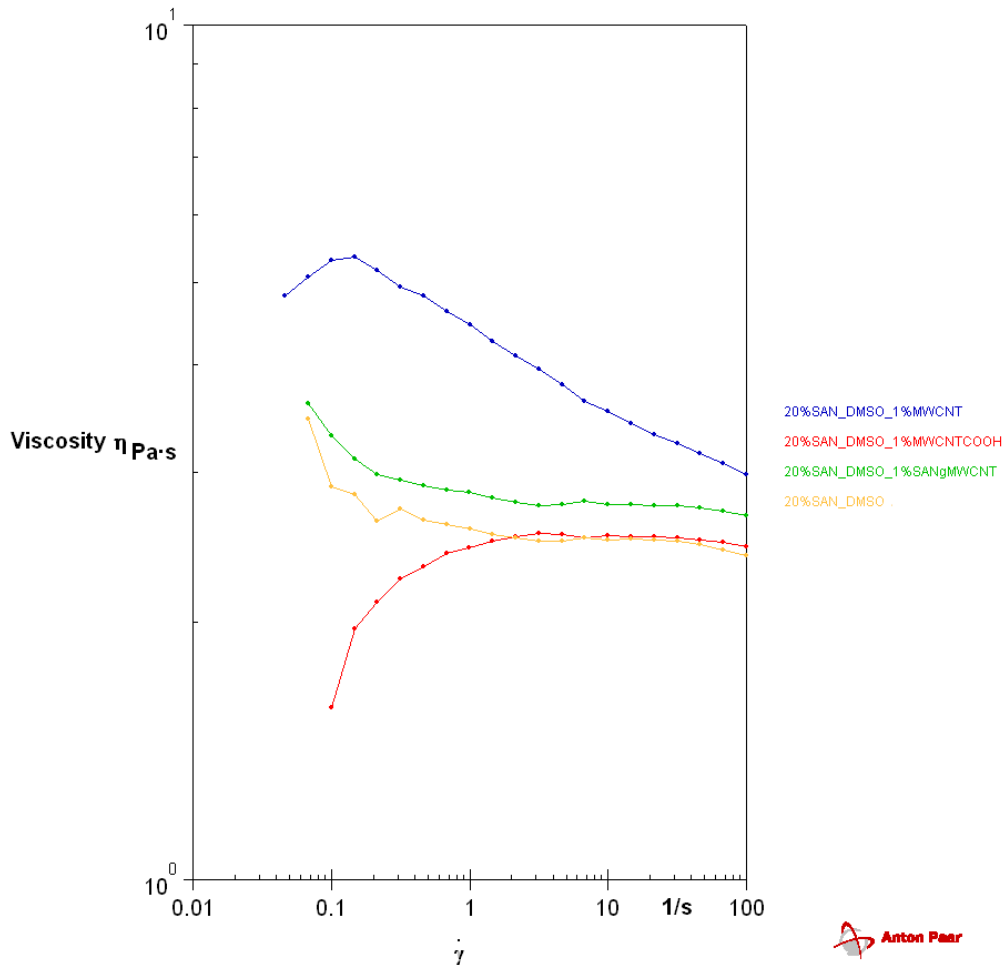
Figure 22. Flow curve of solutions

With 20% SAN in DMSO solution it can be seen on the graph that shear thinning occurs and the curve represents the typical behaviour of Non-Newtonian liquid, which is characteristic for polymer solutions [52, 53]. In addition, 20% SAN in DMSO + 1% MWCNT and 20% SAN in DMSO + 1% MWCNT-COOH solutions curves show typical behaviour of suspensions with shear thinning effect [54]. Furthermore, SAN in DMSO + 1% SANm-g-MWCNT solution curve has typical behaviour of polymer solution due to the grafting process, where nanotubes where coated with polymer.

On figure 23, there are presented solution viscosities at certain shear rates. It can be noted that 20% SAN in DMSO has the smallest viscosity. When to add MWCNTs to the solution, then the viscosity increases, because CNTs develop an interconnecting network in the suspension similar to a gel and invoke a sharp increase in suspension viscosity [55].
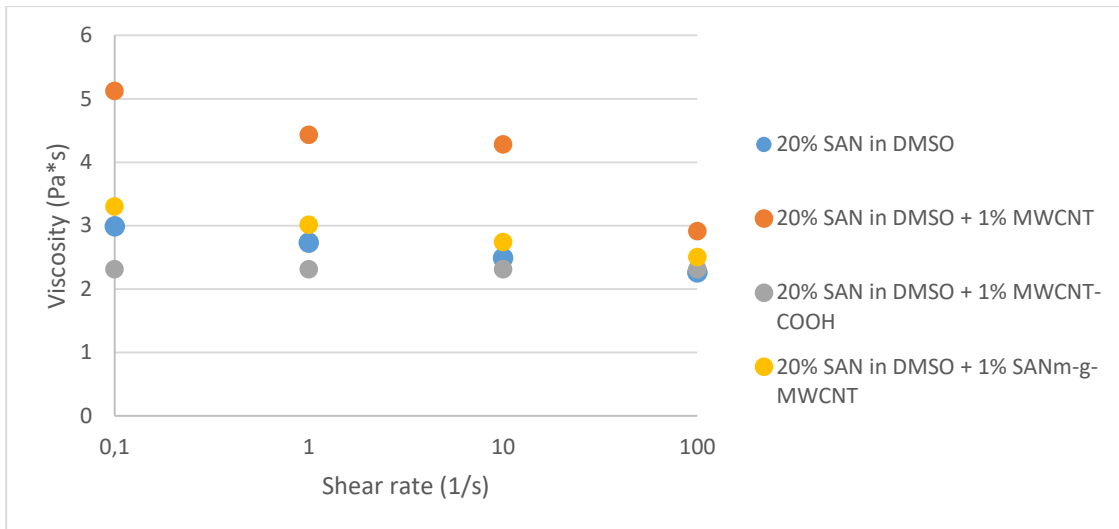
Figure 23. Solution shear rate and viscosity dependence

20% SAN in DMSO + 1% MWCNT-COOH solution has smaller viscosity than solution with MWCNTs, because dispersion is enhanced with functionalized MWCNTs [51]. It can be also noted that 20% SAN in DMSO + 1% SANm-g-MWCNT has smaller viscosity that solution with MWCNTs. This is due to grafting method, where dispersion of nanoparticles in the polymer matrix is improved and also the polymer content on the surface of CNTs is 40%. These reasons effect solution viscosity [24].

4.3 Electrospun fiber analyses

Morphology and mechanical properties of following electrospun mats were analysed: SAN, SAN + 1% MWCNT, SAN 1% MWCNT-COOH and SAN + 1% SANm-g-MWCNT.

4.3.1 Fiber morphology

On figure 24, there are presented the average diameters of electrospun mats. Fiber average diameter of SAN mat is 2098 nm and with adding nanotubes, the diameter of electrospun fiber increases. With SAN + 1% MWCNT fiber average diameter is 2305 nm, which is the biggest diameter of electrospun fibers. 20% SAN in DMSO + 1% MWCNT solution has the highest viscosity of electrospun fiber solutions, which influences the fiber diameter. If there are less charges on the jet and on the solution, then the stretching is weak and due to that the diameter increases [38]. SAN + 1% MWCNT-COOH mats has also lower fiber average diameter compared to the SAN + 1% MWCNT mat. This is also due to the lower viscosity.

With SAN + 1% SANm-g-MWCNT the resulting average diameter is 1204 nm, which is the smallest compared with other electrospun fibers. Compared to SAN + 1% MWCNT mat, this fiber average diameter is two times smaller. With grafting method dispersion of nanoparticles in the polymer matrix is enhanced and this also effects solution viscosity, which is decreased compared to 20% SAN in DMSO + 1% MWCNT [24]. With lower viscosity, fiber average diameter decreases. In addition, SAN in DMSO + 1% SANm-g-MWCNT solution also has high electrical conductivity, which means that there is a bigger stretching of a solution and electrospinning jet can carry more charges and force towards collector increases as well and due to that the fiber diameter decreases [38]. Small diameter is desired due to the excellent properties that nanofibers exhibit (e.g. high tensile strength, large surface area, low density and porous structure) [35].
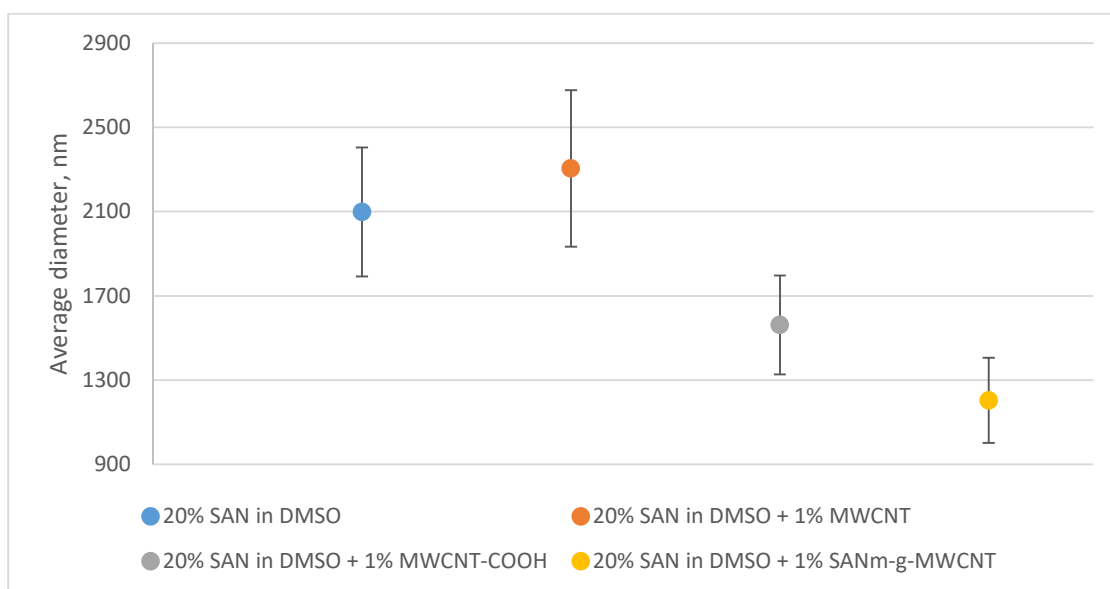

Figure 24. Electrospun fiber average diameter

On figure 25, there are SEM pictures of electrospun mats and single fibers. In case of SAN mats there can be seen several beads along the fiber. These are solvent beads, which have stretched shape. SAN + 1% MWCNT fibers have several big round beads, which is due to CNTs highly agglomerated morphology [24]. In addition, SAN + 1% MWCNT-COOH mats have less beads along the fibers due to MWCNT functionalization with carboxyl group and as a result, there are smaller and less agglomerates. SAN + 1% SANm-g-MWCNT mats have the best morphology of electrospun mats due to improved dispersion of the CNT agglomerates into electrospinning polymer solutions [56].
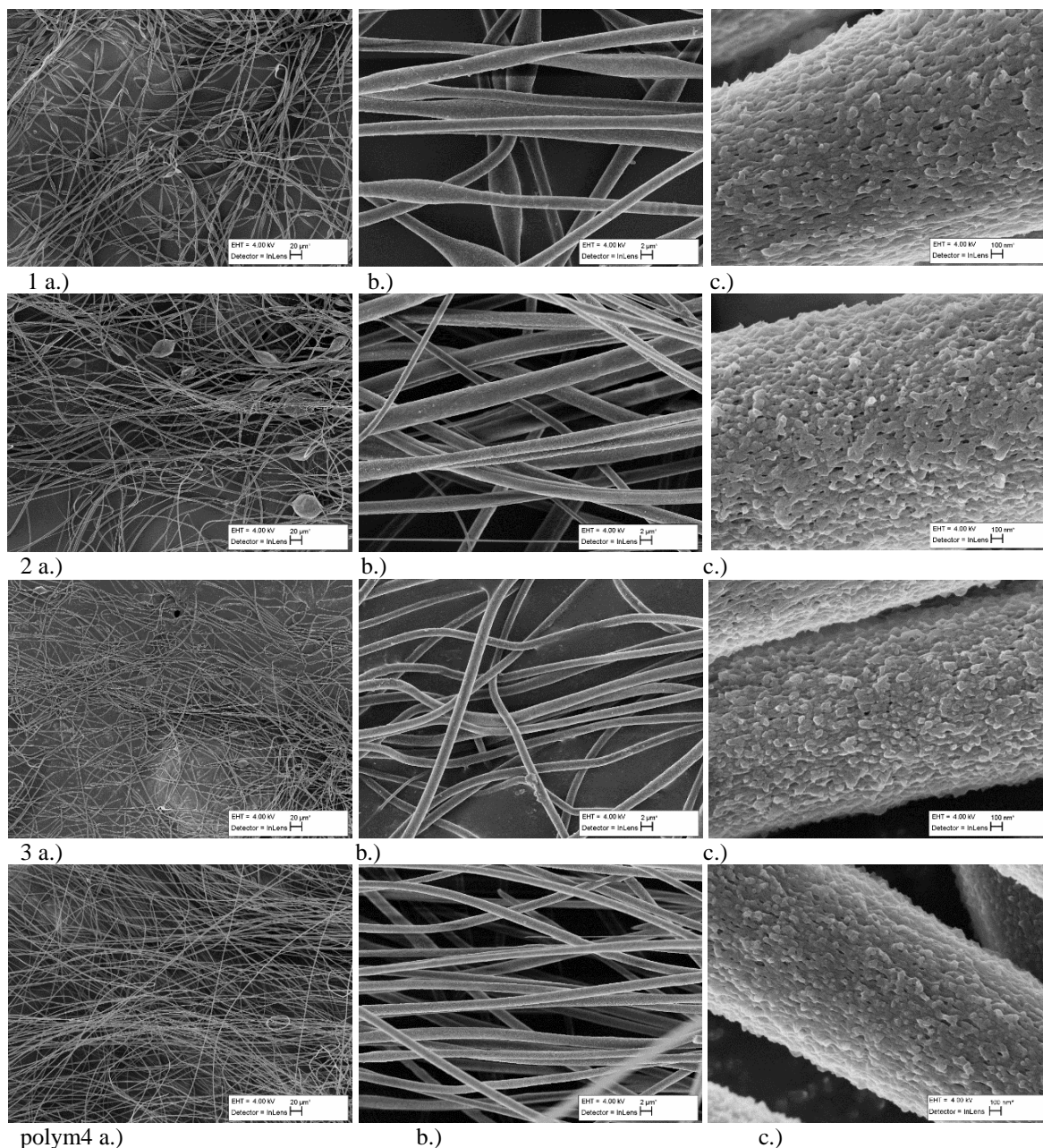
Figure 25. SEM pictures of electrospun fibers 1. SAN 2. SAN + 1% MWCNT 3. SAN + 1% MWCNT-COOH 4. SAN + 1% SANm-g-MWCNT, a.) resolution x500, b.) resolution x2000, c.) resolution x100000

From SEM analysis, it was found that obtained fibres have porous structure. Porous structure means that volume to ratio increases as well. A porous structure composed of nanofibers is a dynamic system, where the pore size and shape can change, unlike conventional rigid porous structures [57]. According to the literature porous fibers can be formed using phase separation [58]. By carrying out electrospinning process with volatile solvent, rapid solvent vaporization occurs and the fiber appears porous as the solvent-rich phase is dried out [59, 60].

In this research, the DMSO was used as a solvent for SAN in electrospinning experiments. Its high boiling point and low evaporation speed make electrospinning of SAN continuous [62, 63]. But as it is a poor solvent for SAN, the porous structure was obtained. It was not the main goal of this research, but as high porosity is desirable in several applications such as healthcare, energy, environmental engineering and biotechnology, defence and security, the potential application field list for obtained mats is wider now due to porous structure of the fiber surface [57, 60, 61].

4.3.2 Mechanical properties of electrospun fibers

Mechanical testing where conducted on electrospun mats, which composition was following: SAN, SAN + 1% MWCNT, SAN + 1% MWCNT-COOH, SAN + 1% SANm-g-MWCNT (see Figure 26, 27, 28).
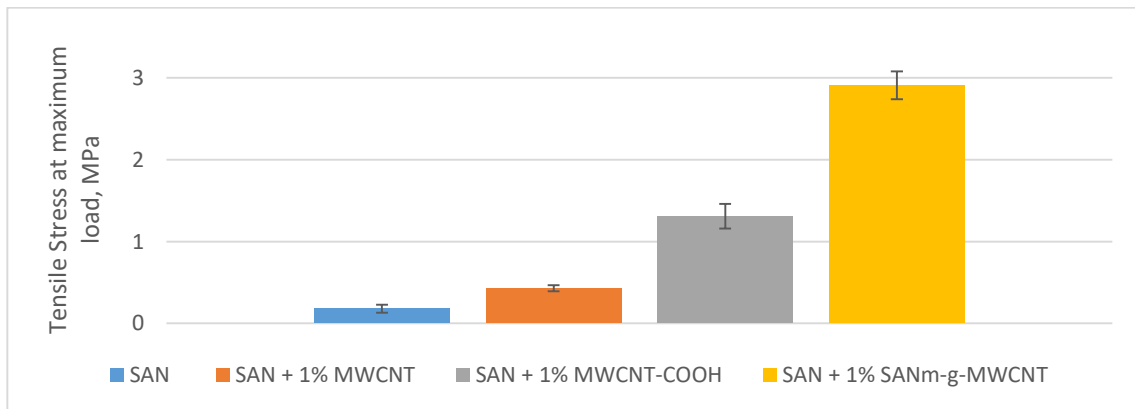

Figure 26. Tensile stress at maximum load of electrospun mats
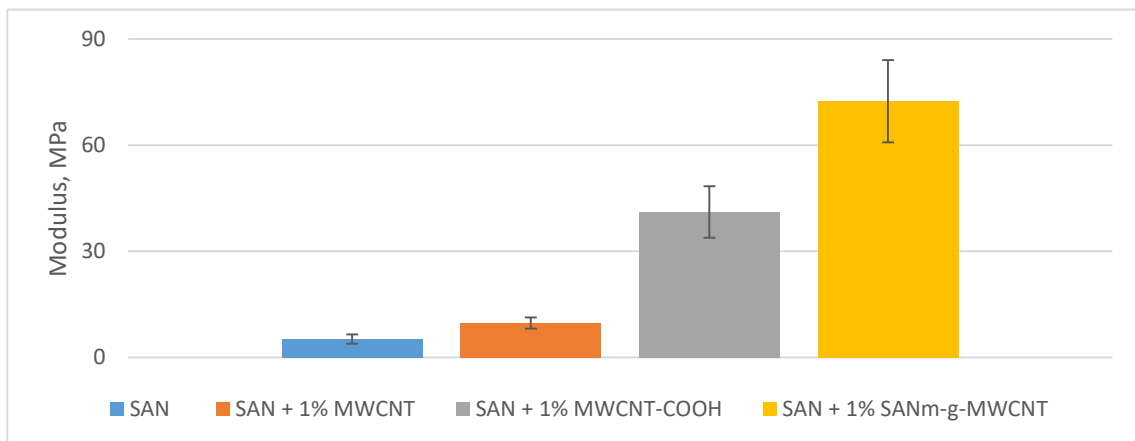

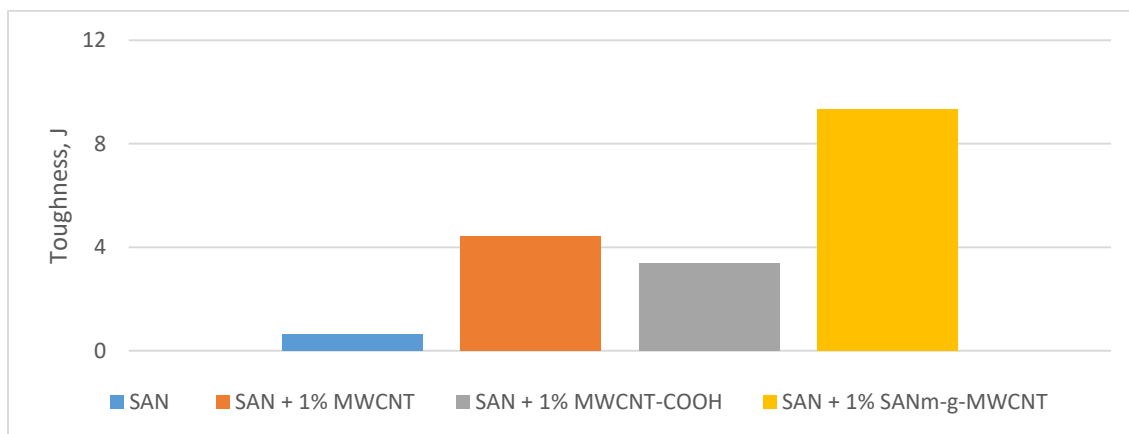Figure 27. Modulus of electrospun mats

Figure 28. Toughness of electrospun mats

The lowest tensile stress at maximum load of mat was 0,18 MPa, which consisted of SAN. Also SAN mat had the lowest modulus and toughness as well. Mats with carbon nanotubes have higher tensile stress than mats spinned with pure polymer solution due to outstanding mechanical properties of CNTs [7].

MWCNT-COOH mat obtained higher tensile stress at maximum load and modulus than mat with MWCNT. According to the literature, all MWCNTs with functional groups provide higher strength than p-MWCNT. This is due to the better dispersion of functionalized MWCNTs [64]. Nanotubes are insoluble in many solvents and polymers, but when to attach physically or chemically functional groups onto CNTs, dispersion increases [65]. Although MWCNT-COOH had higher tensile stress and modulus, calculations showed that toughness is slightly smaller compared to the electrospun MWCNT mat. In case of surface modification of MWCNTs, strong acids such as sulphuric and nitric acids are used in the modification process, when CNTS are functionalized with carboxyl functional group [66]. Due to those acids used in the process, CNTs' sidewalls are damaged and have defects and the original properties of CNTs are changed after modification [67, 68, 69]. Due to MWCNT-COOH damaged surface, toughness of SAN + 1% MWCNT-COOH was smaller compared to electrospun mats with ungrafted nanotubes.

The highest tensile stress at maximum load of mat was 2,91 MPa, which composed of SAN + 1% SANm-g-MWCNT. This mat had also the highest modulus and toughness. Compared to electrospun mat with pure polymer solution, tensile stress increased 16 times with adding SANm-g-MWCNT to the polymer solution. Polymer-nanocomposite membranes have high mechanical stress due to covalently coated nanotubes that have

increased dispersion, which helps to achieve good load transfer to the nanofiller network. This results in more uniform stress distribution, which helps to enhance mechanical properties of the matrix polymer [1, 24].

Conclusion

The results of this thesis can be concluded as satisfactory, because the objective of the research was achieved. It was proven that SAN can be successfully grafted onto surface of MWCNTs by one-step compounding method and dispersion of CNTs was enhanced.

With TGA it was concluded that material loss of SANm-g-MWCNT was 40% and decomposition was between 380-430 °C, which is similar to mass loss curve of SAN and SANm. SANm-g-MWCNT was analysed with ^{1}H-NMR as well. ^{1}H-NMR showed peaks of styrene unit, which shows that polymer is present in the sample.

Solution properties like electrical conductivity and rheology were investigated. 20% SAN in DMSO + 1% SANm-g-MWCNT solution electrical conductivity was 1,60 µS/cm. Although its conductivity was bigger than polymer solutions' conductivity, compared to other solutions with MWCNT and MWCNT-COOH, electrical conductivity is slightly smaller due to grafting process, because CNTs are covered with the polymer. Flow curve of SAN in DMSO + 1% SANm-g-MWCNT solution shows typical behaviour between suspension and polymer solution.

Electrospun fiber analyses showed that SAN + 1% SANm-g-MWCNT mats had the best morphology. There were less beads due to improved dispersion of the CNT agglomerates. SAN + 1% SANm-g-MWCNT had also the smallest fiber average diameter, which was 1204 nm. SEM pictures also showed porous surface. The highest tensile stress at maximum load of mat was 2,91 MPa, which belonged to the SAN + 1% SANm-g-MWCNT electrospun mat. Compared to electrospun mat with SAN, the result was 16 times higher. Due to increased CNT dispersion, stress distribution becomes more uniform and mechanical properties of polymer matrix increase.

For future experiments, electrospinning could be carried out with different grafted carbon nanotube concentrations in a polymer solution. This would show how different concentrations of grafted nanotubes affect the rheological behaviour of solutions and if there is an effect to morphology and to mechanical properties of mats. In addition, to improve electrical properties of electrospun mats, additives such as ionic liquid could be used.

References

1. Shi J.-H., Yang B.-X-, Goh S. H., Covalent functionalization of multiwalled carbon nanotubes with poly(styrene-co-acrylonitrile) by reactive melt blending. European Polymer Journal, 2009, vol 45, 1002-1008.
2. Shanmugharaj A. M., Bae J. H., Nayak R. R., Ryu S., H., Preparation of Poly(styrene-co-acrylonitrile)-Grafted Multiwalled Carbon Nanotubes via Surface-Initiated Atom Transfer Radical Polymerization. Journal of Polymer Science, 2006, vol 45, 460–470.
3. Choi W. S., Ryu S., H., Enhancement of Dispersion of Carbon Nanotube and Physical Properties of Poly(styrene-co-acrylonitrile)/ Multiwalled Carbon Nanotube Nanocomposite via Surface Initiated ATRP. Journal of Applied Polymer Science, 2010, vol 116, 2930–2936.
4. Liu P., Modifications of carbon nanotubes with polymers. European Polymer Journal, 2005, vol 45, 2693–2703.
5. G.Wypych. Handbook of polymers. Canada, Toronto: GhemTec Publishing, 2012.
6. Bitenieksa J., Meria R. M., , Zicansa J., Maksimovsb R., Vasilec C., Musteatac V.E., Styrene–acrylate/carbon nanotube nanocomposites: mechanical, thermal, and electrical properties. Proceedings of the Estonian Academy of Sciences, 2012, vol 61, 172-177.
7. Spitalsky Z., Tasis D., Papagelis K., Galliotis C., Carbon nanotube–polymer composites: Chemistry, processing, mechanical and electrical properties. Progress in Polymer Science, vol 5, 2009, 357-401.
8. Scopus. [WWW] https://www.scopus.com/home.uri (25.03.2017)
9. Pantano A., Carbon Nanotube Based Composites - Processing, Properties, Modelling and Application, Smithers Rapra Technology, 2012, 49-164.
10. Eatemadi A., Daraee H., Karimkhanloo H., Kouhi M., Zarghami N., Akbarzadeh A., Abasi M., Hanifehpour Y., Joo S., W., Carbon nanotubes: properties, synthesis, purification, and medical applications, Eatemadi et al. Nanoscale Research Letters 2014, 9:393, 1-13.
11. CNT properties. [WWW] http://www.sigmaaldrich.com/technical-documents/articles/materials-science/single-double-multi-walled-carbon-nanotubes.htm (14.04.2017)
12. CNT properties [WWW] http://www.nanoscience.com/applications/education/overview/cnt-technology-overview/properties-applications-carbon-nanotubes/ (14.04.2017)
13. Saito, R., Dresselhaus, G., Dresselhaus, MS., Physical Properties of Carbon Nanotubes. World Scientific, 1998.
14. Ken D., Craig P., Rodger D., James B. Toxicology of Carbon Nanotubes. Cambridge University Press, 2012, 1-3.
15. Harris P. Carbon Nanotube Science - Synthesis, Properties and Applications. Cambridge University Press, 2009, 179- 292.

16. Khan W., Sharma R., Saini P., Carbon Nanotube-Based Polymer Composites: Synthesis, Properties and Applications. Intech open science, 2016, 1-45.

17. Beyou E., Akbar S., Chaumont P., Cassagnau P.,mPolymer Nanocomposites Containing Functionalised Multiwalled Carbon NanoTubes: a Particular Attention to Polyolefin Based Materials. Intech, 2013, 77-81.

18. Fengge G. Advances in Polymer Nanocomposites 1st Edition Types and Applications. Woodhead Publishing, 2012, 184.

19. Conjugated polymers. [WWW] http://plasticphotovoltaics.org/lc/lc-materials/lc-conjugated.html (25.03.2017)

20. Samanta S., Fritsch M., Scherf U., Gomulya W., Bisri S., Lo M., Conjugated Polymer-Assisted Dispersion of Single-Wall Carbon Nanotubes: The Power of Polymer Wrapping. American Chemical Society, 2014, 47 (8), 2446–2456.

21. Kymakis E., Amaratunga G. A. J, Single-wall carbon nanotube/conjugated polymer photovoltaic devices. American Institute of P/Fhysics, 2002, vol 80, 112.

22. Kar K., Pandey J., Rana S., Handbook of Polymer Nanocomposites. Processing, Performance and Application. Volume B: Carbon Nanotube Based Polymer Composites. Springer-Verlag Berlin Heidelberg, 2015, 105-108.

23. Tasis D., Carbon Nanotube-polymer Composites. Royal Society of Chemistry, 2013, 255.

24. Bhattacharya M., Polymer Nanocomposites—A Comparison between Carbon Nanotubes, Graphene, and Clay as Nanofillers. MDPI, 2016, 9, 1-10.

25. Du J-H., Bai J., Cheng H-M., The present status and key problems of carbon nanotube based polymer composites. eXPRESS Polymer Letters Vol.1, 2007, vol 5, 253-273.

26. CNT-polymer composite applications. [WWW]. https://sites.google.com/site/cntcomposites/cnt-polymer-applications (25.03.2017)

27. Koyama S., Haniu H., Osaka K., Koyama H., Kuroiwa N., Endo M., Kim Y.A., Hayashi T., Medical application of carbon-nanotube-filled nanocomposites: the microcatheter. Small, 2006, vol 2(12):1406-11.

28. Cirillo G., Hampel S., Spizzirri U.G., Parisi O.I, Picci N., Iemma F., Carbon Nanotubes Hybrid Hydrogels in Drug Delivery: A Perspective Review, BioMed Research International, 2014, Volume 2014, 1-17.

29. Huber T.A., Polymer-Carbon Nanotube Composites. Defence R&D Canada – Atlantic Technical Memorandum, 2004, 1-9.

30. Properties of SAN. [WWW]. http://www.patterson-rothwell.co.uk/images/services/materialinformation.pdf (26.03.2017)

31. Tucker, N., Stanger, J., Staiger M., Razzaq H., Hofman K., The History of the Science and Technology of Electrospinning from 1600 to 1995. Journal of Engineering Fibers and Fabrics, 2012.

32. Nascimento M.L., Araújo E.S., Cordeiro E.R., de Oliveira A.H., de Oliveira H.P., A Literature Investigation about Electrospinning and Nanofibers: Historical Trends, Current Status and Future Challenges, Recent Pat Nanotechnol, 2015, vol 9(2), 76-85

33. Agarwal S., Burgard M., Greiner A., Wendorff J., Electrospinning: A Practical Guide to Nanofibers, alter de Gruyter GmbH & Co KG, 2016, 33

34. Kurban Z., Lovell A., Bennington S., Jenkins D., Ryan K., Jones M., Skipper N., David W., A Solution Selection Model for Coaxial Electrospinning and Its Application to Nanostructured Hydrogen Storage materials. The Journal of physical chemistry, 2010, 114 (49), 21201–21213.

35. Huanga Z., Zhangb Y., Kotakic M., Ramakrishn S., A review on polymer nanofibers by electrospinning and their applications in nanocomposites.Composites Science and Technology, 2003, 63, 2223–2253.

36. Electrospinning process. [WWW] http://www.sisweb.com/referenc/articles/kds-issue1001.pdf (29.03.2017)

37. Electrospinning apparatus. [WWW] http://www.scielo.br/img/revistas/bjce/v26n1/a06fig01.jpg (06.02.2017)

38. Ramakrishna S., Fujihara K., Teo W., Lim T., Ma, Z., An introduction to electrospinning and nanofibres. World Scientific Publishing Co. Pte. Ltd., 2005, 90-116

39. Polymer solution. [WWW] http://encyclopedia2.thefreedictionary.com/Polymer+Solution (06.02.2017)

40. Polymer Molecular Weight. [WWW] http://chemistry.about.com/od/chemistryglossary/g/Molecular-Weight-Definition.htm (06.02.2017)

41. Qin. Y., Micro-Manufacturing Engineering and Technology, Elsevier, 2010, 220-222.

42. Hu. J., Adaptive and Functional Polymers, Textiles and their Applications, World Scientific, 2011, 268-270.

43. Li Z., Wang C., One-Dimensional nanostructures, SpringerBriefs in Materials, 2013, 15-28.

44. Collector. [WWW] http://electrospintech.com/collector.html#.WK1Cn2996M8 (22.02.2017)

45. Radhi, M., M., Tan W., T., Rahman. M., Z., B., Kassim, A., B. Synthesis and characterization of grafted acrylonitrile on polystyrene modified with activated carbon using gamma-irradiation. Scientific Research and Essays, 2012, Vol. 7(7), 790-795.

46. Ma Y., Pang Y., Mechanism Study on Char Formation of Zinc Acetylacetonate on ABS Resin. Chinese Journal of Polymer Science, 2015, 33(5): 772-782.

47. Sadegh H., Zare K., Maazinejad B., Shahryari-ghoshekandi R., Tyagi I., Agarwal S., Gupta V., Synthesis of MWCNT-COOH-Cysteamine composite and its application for dye removal. Journal of Molecular Liquids, 2016, vol 215, 221–228.

48. Li Z., Wang C., One-Dimensional nanostructures Electrospinning Technique and Unique Nanofibers. Springer-Verlag Berlin Heidelberg, 2013, 15-28.

49. Aguilar J. O., Bautista-Quijano J.R., , Avilés F., Influence of carbon nanotube clustering on the electrical conductivity of polymer composite films. eXPRESS Polymer Letters, 2010, Vol.4, No.5, 292–299.

50. Lima A., Castro V., Borges R., Silva G., Electrical Conductivity and Thermal Properties of Functionalized Carbon Nanotubes/Polyurethane Composites. Departamento de Química, UFMG, 2012, vol 22, 117.

51. Lee J., Kim M., Hong C., K., Shim S. E., Measurement of the dispersion stability of pristine and surface-modified multiwalled carbon nanotubes in various nonpolar and polar solvents. Measurement science and technology, 2007, vol 18, 3707–3712

52. Schramm G., A practical approach to rheology and rheometry 2nd edition. Gebrueder Haake, 1998, 11-24.

53. Viscosity of Newtonian and non-Newtonian Fluids. [WWW] http://www.rheosense.com/applications/viscosity/newtonian-non-newtonian (22.02.2017)

54. Yearsley K., Mackley M., Chinesta F., Leygue A., The rheology of multiwalled carbon nanotube and carbon black Suspensions. Journal of Rheology, 56(6), 2012, 1465-1490.

55. Fan Z., Advani S. G., Rheology of multiwall carbon nanotube suspensions. The Society of Rheology, Inc, 2007, 51(4), 585-604

56. Polymer nanocomposites based on carbon nanotubes. [WWW] https://www.politesi.polimi.it/bitstream/10589/56691/1/2012_02_PhD_Molina.p df (26.03.2017)

57. Esfandarani M.S, Johari M.S., PRODUCING POROUS NANOFIBERS. Nanocon2010, 2010.

58. Ramakrishna S., Fujihara K, Teo1 W.E., Yong T., Ma Z., Ramaseshan R., Electrospun nanofibers: solving global issues. MaterialsToday, 2006, vol 9, 40-50.

59. Porous/Dimpled/Pitted Fibers. [WWW] http://electrospintech.com/porousfiber.html (11.03.2017)

60. Dayal P., Kyu T., Porous fiber formation in polymer-solvent system undergoing solvent evaporation. Journal of Applied Physics, 100, 2006, 043512-1.

61. Katsogiannis K.A.G,, Vladisavljević G.T, Stella G., Porous electrospun polycaprolactone (PCL) fibres by phase separation. Macromolecular Nanotechnology, 2015, volume 69, 284–295.

62. Evaporation Rates at Specified Conditions. [WWW] http://www.jysco.com/archives/Biotage/TurboVap_96/TurboVap_96_evaporatio n_rate.pdf (06.04.2017)

63. DMSO Physical Properties. [WWW] http://www.gaylordchemical.com/products/literature/dmso-physical-properties (06.04.2017)

64. Eren O., Ucar N., Onen A., Karacan I., Kizildag N., Demirsoy N., Vurur O., Borazan I., Effect of differently functionalized carbon nanotubes on the properties of composite nanofibers. Indian Jorunal of Fibre & Textile Research, vol 41, 2016, 138-144.

65. Carbon Nanotubes, Dispersion and Functionalization of Carbon Nanotubes from Cheap Tubes. [WWW] http://www.azonano.com/article.aspx?ArticleID=1563 (26.03.2017).

66. Turgunov M., A., Oh J., Yoon S., H., Surface Modification of Multiwall Carbon Nanotubes by Sulfuric Acid and Nitric Acid. Advanced Science and Technology Letters, vol.64, 2014, 22-25.

67. Le V., T., Ngo C., L., Le Q., T., Ngo T., T., Surface modification and functionalization of carbon nanotube with some organic compounds. Adv. Nat. Sci.: Nanosci. Nanotechnol., vol 4, 2013, 1-5.

68. Wepasnick K.A, Billy A. Smith B., A., Kaitlin E. Schrote K., E., Hannah K. Wilson H., K., Diegelmann S., R., Fairbrother D., H., Surface and structural characterization of multi-walled carbon nanotubes following different oxidative treatments. Carbon, vol 49, 2011, 24-36.

69. Marshall M., W., Popa-Nita S., Shapter J., G., Measurement of functionalised carbon nanotube carboxylic acid groups using a simple chemical process. Carbon, vol 44, 2006, 1137–1141.

70. Fulmer G., R., Miller A., J., M., Sherden N., H., Gottlieb H., E., Nudelman A, Stoltz B., M., Bercaw J., E., Goldberg K., I, NMR Chemical Shifts of Trace Impurities: Common Laboratory Solvents, Organics, and Gases in Deuterated Solvents Relevant to the Organometallic Chemist. Organometallics, vol 29, 2010, 2176–2179.

Acknowledgements

Summary

The objective of this research is to enhance dispersion of carbon nanotubes (CNT) with the purpose of transmitting CNTs good mechanical properties into poly(styrene-co-acrylonitrile) (SAN) matrix in electrospun fibers. For this, a new method for covalent bonding between MWCNT-COOH and SANm had to be invented to achieve the best dispersion of CNTs.

Firstly, to form modified SAN, polymer was mixed in a compounder with a catalyst and as a result, cyano groups were converted into oxazoline group. After modification, multi-walled carbon nanotubes with carboxyl groups (MWCNT-COOH) were added into the compounder and mixed for some time with modified polymer. Finally, polymer grafted carbon nanotubes were extruded from the compounder. During this research one-step method for covering carbon nanotubes with polymer was developed.

Both TGA and ^{1}H-NMR showed that with one-step compounding method it was possible to make polymer grafted carbon nanotubes. Furthermore, different solutions were prepared and rheological behaviour and electrical conductivity was investigated. Results showed that dispersion of CNTs was improved with grafting process.

Furthermore, electrospinning was carried out with the purpose of forming mats with fine morphology and high mechanical strength. After electrospinning mechanical properties of mats were investigated. Mats, which consisted of grafted material, had the best mechanical properties. SEM showed that mats with SANm-g-MWCNT had the smallest average diameter and fibers had only few beads and a porous surface.

In conclusion, this research was successful because with innovative one-step compounding method, SAN was grafted onto the surface of MWCNTs and a strong covalent bond was achieved. All results showed that CNT dispersion was enhanced as well.

Kokkuvõte

Lõputöö eesmärk on süsiniknanotorude dispersiooni parendamine eesmärgiga üle kanda nanotorude head mehaanilised omadused polü(stüreen-ko-akrüülnitriil)-i polümeeri maatriksisse. Selle saavutamiseks oli vaja välja töötada innovaatiline meetod polümeeri ja karboksüülrühmaga nanotorude kovalentseks sidumiseks.

Kõigepealt polümeeri modifisteerimeseks segati kompaunderis polümeer katalüsaatoriga, mille tulemusel tsüano funktsionaalne grupp muudeti oksazoliin grupiks. Pärast polümeeri modifitseerimist lisati kompaunderisse karboksüülrühmaga süsiniknanotorud ning lasti materjalidel seguneda. Selle protsessi tulemusel saavutati kovalentne side modifitseeritud polümeeri ja karboksüülrühmaga süsiniknanotorude vahel ning töötati välja üheastmeline meetod süsiniknanotorude katmiseks polümeeriga.

Nii TGA kui ka ^{1}H-NMR analüüs näitasid, et üheastmelise kompaundimise meetodiga toimus edukas nanotorude katmine polümeeriga. Järgnevalt valmistati lahused, mille reoloogilist käitumist ja elektrilisi omadusi uuriti. Need tulemused näitasid, et kovalentse sidumise teel paranes nanotorude dispersioon.

Valmistatud lahuseid kasutati elektroketrusprotsessi läbi viimiseks. Meetodi tulemusel saadi suurepärase morfoloogia ja heade mehaaniliste omadustega matid. Erinevaid matte analüüseeriti ning tõmbekatsed näitasid, et mattidel, mille puhul kasutati SANm-g-MWCNT materjali, mehaanilised tugevused olid kõige paremad. Lisaks ka kiu keskmine diameter oli kõige väiksem ja kiude struktuur oli poorne ning väheste lahusti mullidega.

Kokkuvõtteks, uurimistöö oli väga edukas, sest töö käigus töötati välja innovaatiline üheastmeline kompaundimise meetod ning moodustati tugev kovalentne side polümeeri ja karboksüülrühmaga nanotorude vahel. Lahuse parameetrite analüüs ning mattide analüüs näitasid ka seda, et paranes süsiniknanotorude dispersioon.